

# Synchronization and fractal scaling as foundations for cognitive control

Mary Jean Amon<sup>a</sup>, Olivia C. Pavlov<sup>b</sup> & John G. Holden<sup>b\*</sup>

<sup>a</sup> Developmental Cognitive Neuroscience Laboratory, Department of Psychological and Brain Sciences, 1101 East Tenth Street, Indiana University Bloomington, Bloomington, Indiana, 47405, United States of America

<sup>b</sup> The Complexity Group, Department of Psychology, University of Cincinnati, PO Box 210376, Cincinnati, Ohio, United States of America

\*Corresponding author

E-mail: john.holden@uc.edu (JGH)

Declarations of interest: None.

This is a PDF file of a published manuscript. Please consult the published source for citations and quotes.

Please cite as:

Amon, M. J., Pavlov, O. C., & Holden, J. G. (2018). Synchronization and fractal scaling as foundations for cognitive control. *Cognitive Systems Research*, 50, 155-179. doi: <https://doi.org/10.1016/j.cogsys.2018.04.010>.

**Abstract**

This article investigates the degree to which the intrinsic propensity for entrainment in oscillatory systems serves as a plausible foundation for understanding the assembly and flexibility of cognitive systems. Three experiments tested for the strength of performance entrainment to oscillations inserted into event timing and stimulus properties of cognitive tasks. In the first temporal estimation experiment, attractor strength analyses revealed participants spontaneously entrained to sinusoidal changes in the duration of inter-trial intervals. A second simple reaction time task introduced oscillatory changes to the inter-stimulus interval durations across trials, and attractor strength analyses revealed weaker but reliable entrainment to the input signals. A third dyadic temporal estimation task revealed oscillatory entrainment that was distributed across pairs of participants. The experimental results were evaluated in terms of coupled oscillator dynamics and short-term perceptual lags. The entrainment hypothesis was most successful in explaining the empirical patterns, suggesting that cognitive performance relies on coordinative activity. Together, the three studies demonstrated coordinative activity over a range of temporal scales and distributed across individuals comprising the dyads. The simple reaction time study illustrated within-trial coordinative dynamics; individual temporal estimation illustrated across-trial coordination, and dyadic temporal estimation illustrated person-to-person coordinative dynamics. The findings underscore the role environmental constraints impose on cognitive activity and demonstrate how seemingly disparate features of distinct cognitive tasks can be assimilated in terms of synchronization principles.

*Keywords:* Cognitive dynamics; distributed cognition; entrainment;  $1/f$  scaling.

## 1. Introduction

Understanding the organization of cognitive systems requires consideration of how their component processes become functionally linked, allowing them to behave as unified systems. Historically some of the most clearly articulated descriptions of coordinative activity arose in the study of non-living systems that express the dynamics of coupled oscillators (Huygens, 1673/1986; Newton, 1686/1729). Equations describing the dynamics of coupled pendula served as entry points for successful models of motor coordination, especially human locomotion (Haken, Kelso, & Bunz, 1985; Kelso, 1995; Kugler, & Turvey, 1987; Schöner, Haken, & Kelso, 1986; Thelen & Smith, 1994; von Holst, 1939/1973). The resulting models reliably predict numerous details of the dynamics and relative phase relations expressed during rhythmic movement by both real and virtual limbs. The physical analogy between an oscillating pendulum and limb flexion during locomotion is easy to recognize: pendula and limbs are both pivot-anchored, entail mass, and their lengthwise spatial extents are oriented perpendicular to the force of gravity.

It is less obvious that oscillator dynamics also deliver coherence to the domain of computational neuroscience. For instance, introductory texts often portray the behavior of individual neurons in relatively simple binary terms: they fire action potentials and otherwise occupy a resting-potential state. Similarly, the net neurochemical effects of neurotransmitters are said to be either excitatory or inhibitory. In fact, neurons express a broad range of periodic electrophysiological patterns that are aptly characterized in terms of linear and nonlinear oscillator dynamics (e.g., see Buzsáki, 2006; Glass, 2001; Izhikevich, 2007).

The nervous system expresses rich and varied patterns of spatiotemporal coordination. Oscillatory dynamics are now broadly implicated as the basis for recruiting, maintaining, and resetting cortical and subcortical networks involved in guiding and controlling behavior (Buzsáki & Draguhn, 2004; Fries, 2015; Helfrich & Knight, 2016). Rhythmic transcranial magnetic stimulation studies established a capacity to influence perception, memory, and response time performance by manipulating coordinative brain dynamics (Thut, Miniussi, & Gross, 2012). Elementary cognitive activities inhabit timescales of change that fall in-between those of very fast electrophysiological dynamics and slower, ongoing movement dynamics. Thus, oscillatory phenomena may constrain the organization and expression of cognitive activity in general.

This article applies synchronization principles to cognitive performance by examining coordination expressed across two elementary cognitive activities: temporal estimation and simple reaction time. Both tasks are traditionally thought to emphasize largely distinct cognitive functions. Temporal estimation requires high-level timekeeping-relevant cognitive functions. By contrast, simple reaction time emphasizes perceptual-motor thresholds and imposes minimal high-level cognitive loads. However, when viewed through the lens of entrainment dynamics, both tasks display coordinative patterns in their organization and commonalities such as frequency detuning, that are uniquely predicted by oscillator dynamics.

Techniques derived from the generalized mathematics of oscillatory systems are employed to study the coordination among processes supporting cognitive performance. Along the way, we establish a strategy for characterizing cognitive

systems that are comprised of dynamically coupled processes. The framework illustrates a novel approach to providing unifying accounts of seemingly distinct cognitive tasks and activities. Next, we briefly introduce several core coordinative concepts that guide our experimental manipulations and statistical analyses.

### 1.1 Grounding cognitive performance in oscillatory dynamics

A dynamic system's state space is the complete set of all potential locations or trajectories the system *could* occupy. Within a state space, "attractors" represent a preferred trajectory or location of a temporally evolving system. Essentially, attractors delimit subsets of a system's state space that it tends to occupy. Give a rocking chair a single push and it will oscillate back and forth until it eventually arrives at a resting state. As such, the point depicting the chair's at-rest position is where it has zero velocity and is a point attractor. More elaborate force-driven systems are typically attracted to a preferred trajectory rather than a point. That is, if they are perturbed, they tend to return to a definite trajectory. For instance, the trajectory of a clock-pendulum will gradually return to normal following a slight disturbance.

Periodic oscillators may be attracted to a particular trajectory within a state space. Two or more oscillators may become synchronized, or dynamically attracted, with one another and entrain to a common phase over time. An oscillator's phase refers to its position in its oscillatory cycle. Two oscillators are said to be in-phase if they occupy identical positions in their cycle, at the same time. Out-of-phase oscillators occupy different positions in their cycle at a given point in time. Phase differences are quantified with an angular measure of the discrepancy, often using degrees. For example, a  $180^\circ$  relative phase difference indicates two oscillators that occupy opposite positions in their respective cycles at a given point in time. The concepts of synchronization via phase locking and attractor dynamics were fleshed out with the help of idealized mathematical frameworks.

Biological systems rarely express strictly regular oscillatory behavior. Instead, they may express quasi-regular fluctuations that entail significant stochastic influences. Nevertheless, attractors and synchronization concepts can be usefully applied to these systems. For example, self-similar fractal patterns of variability (i.e.,  $1/f$  scaling) are present in a variety of cognitive activities that unfold over time and are symptomatic of coordinative activity that is subject to significant stochastic influences. Long-range correlation in the form of  $1/f$  scaling is associated with complex systems whose components self-organize their behavior across multiple temporal or spatial scales (Jensen, 1998). The fact that  $1/f$  scaling conforms to an inverse power-law scaling relation means it is composed of nested, self-similar, and loosely coordinated fluctuations, ranging in duration from very short to very long.

Self-organizing physical, chemical, and biological systems often give rise to  $1/f$  scaling in their patterns of temporal evolution—this same pattern of variation is well established in cognitive performance (e.g., Gilden, Thornton, & Mallon, 1995; Gilden, 2001; 2009; Van Orden, Holden, & Turvey, 2003; 2005). The widely expressed patterns of  $1/f$  scaling in cognitive performance implicate oscillatory coupling as a potentially general feature of cognition (Wijnants, Cox, Hasselman, Bosman, & Van Orden, 2012). There are, of course, competing explanations for the basis of  $1/f$  scaling in cognition. However, the one that has gained the most traction in predicting new phenomena is the hypothesis equating  $1/f$  scaling with interdependent coordinative activity across many

temporal scales (Holden, Choi, Amazeen, & Van Orden, 2011; Kello, Beltz, Holden, & Van Orden, 2007; Kello et al., 2010; Kiefer, Riley, Shockley, Villard, & Van Orden, 2009; Stephen, Arzamarski, & Michaels, 2010; Van Orden et al., 2003; Van Orden, Hollis & Wallot, 2012; Van Orden, Kloos, & Wallot, 2011; Wijnants, Bosman, Cox, Hasselman, & Van Orden, 2009).

An open question and important concern of this article is the basis for  $1/f$  scaling in cognitive activity. One hypothesis claims it originates from *independent* processes that happen to express a scaling relation (e.g., Wagenmakers, Ferrell, & Ratcliff, 2004; 2005; Ward, 2002). An alternative hypothesis claims  $1/f$  scaling is symptomatic of coupling, coordination, and accommodation among *interdependent* processes that span a wide swath of timescales (e.g., Gibbs, 2005; Rigoli, Holman, Spivey, & Kello, 2014; Van Orden et al., 2003; 2005). If coordinative dynamics influence cognitive performances, then it is plausible to propose that  $1/f$  scaling is a consequence of a general coordinative capacity that traverses a wide range of temporal and spatial scales of biological, neurophysiological, and bodily change. One way to discriminate between these two alternatives is to manipulate the coupling between participant and task in a manner that reveals the mode by which task coordination is achieved.

If coordination among mind, body, and task is achieved only by short-term error-corrections that leverage the immediate trial-by-trial stimulus-response task history, then it is plausible to propose that only basic internal perceptual models of the immediate past are required to characterize performance. Cognitive theories that rely on local, contemporaneous information exchanges among dedicated and discrete perceptual processes favor this *independent process* hypothesis (Torre, Varlet, & Marmelat, 2013).

Alternatively, cognitive theories that rely on *oscillatory entrainment* imply a more general capacity for both local and non-local synchronization among perceptual and cognitive processes (Glass, 2001; Helfrich, & Knight, 2016; Izhikevich, 2007; Stephen, Stepp, Dixon, & Turvey, 2008). That is, if cognitive activity relies on coordinative principles to subsume and accommodate oscillatory test signals, then oscillatory principles may support a general capacity for multi-scale stochastic synchronization among physiological and cognitive processes in the form  $1/f$  scaling. Notably, the prospective control literature distinguishes the same local versus global control dichotomy using the terms weak anticipation, indicating short-term error correction, and strong anticipation, indicating non-local interdependence (Stepp & Turvey, 2010).

Next, three studies each test for entrainment to sinusoidal signals during cognitive tasks in order to examine the degree to which cognitive activity expresses coordination to environmental constraints. The key manipulations introduced sinusoidal oscillations to the trial-event timing of temporal estimation and response time tasks. First, a sinusoidal pattern of progressively shorter and then longer inter-trial intervals (ITIs) was built into blank screen downtime between trials in the temporal estimation task. Following that, an identical oscillating sequence of inter-stimulus intervals (ISIs) was inserted into the blank screen duration between the fixation stimulus and the response stimulus in a button-press simple reaction time task. Lastly, a sine wave was interleaved with constant ITIs and presented to one of two individuals that took turns responding in a dyadic temporal estimation task. Statistical analyses were aimed at detecting the degree to which participants' performances relied either on short-term sensory stores, or entrainment with the embedded sinusoidal signals.

## 2. Experiment 1: Sinusoidal synchronization in temporal estimation

Temporal estimation tasks encourage participants to “become a clock” by pressing a button each time a pre-specified time-interval has elapsed. On one hand, a temporal estimation trial-series can be viewed as a series of independent estimates of the same time interval. However, the widely reported presence of  $1/f$  scaling in temporal estimation sequences suggests that quasi-regular fluctuations across a range of timescales support cognitive performance (Buzsáki, 2006; Tognoli & Kelso, 2014a; 2014b; Van Orden et al., 2003). If so, then participants should be able to entrain these oscillatory processes to regular signals in the environment.

This initial study used a temporal estimation task to investigate how intrinsic patterns of fluctuation combine with extrinsic patterns of variability entailed in the laboratory protocol. To accomplish this, a regular oscillation was inserted into the intervals of “down-time” between the successive trials in the temporal estimation task (see also Holden et al., 2011).

There are several core temporal estimation protocols. A *self-paced* protocol imposes minimal extrinsic task demands, by allowing participants to freely press a response key each time they believe a specified interval of time elapsed. The same key-press, in turn, serves as the onset of the next interval to be estimated, and so on. Self-paced protocols generally yield the most robust  $1/f$  signals (Holden et al., 2011).

Relative to self-pacing, a *trial-paced* protocol introduces a predictable source of environmental constraint. In the case of a trial-paced protocol, participants begin their temporal estimation after a particular signal is presented, and the participant responds when they think the specified interval of time has passed. Each response initiates a fixed interval of “down time” before the next signal is presented. In this case, an ITI is the blank-screen downtime between trials, or the time between the last response and start signal of the next trial. While many studies use a fixed ITI, a random ITI unpredictably varies the downtime between successive trials but is subject to a specified mean and standard deviation. In contrast, the present study used a trial-paced protocol and introduced *sinusoidal* patterns of change in the successive ITIs.

The study was comprised of a baseline constant ITI condition and four conditions with variable ITIs. Three experimental conditions introduced different sinusoidal patterns of ITI oscillation: 1) A low-frequency (LF) ITI sine cycles every 20 trials, 2) A high-frequency (HF) ITI sine cycles every 8 trials, and 3) a both-frequencies sine (BF) superposes the HF and LF ITI sine waves. A second control condition randomly presented the individual ITIs that comprised the BF sum-of-sines condition. Inserting unpredictable sources of ITI variability to trial-paced temporal estimation is known to “whiten”, or de-correlate the observed  $1/f$  scaling, relative to a fixed ITI (e.g., Experiment 4, Holden et al., 2011). All the variable ITI conditions shared a 700ms mean and a 180ms standard deviation. In each condition, participants were asked to press the response button when they believed the stimulus had been displayed for seven-tenths of a second (700ms). Two dependent measures were collected during each trial, including the time elapsed during each of our participant’s temporal estimates, and their dwell time on the response button—the time elapsed from key-press to key-release (i.e., *key-press duration*; Kello et al. 2007).

Our prediction was that slowly changing regular oscillations in the timing of the task events would induce performance entrainment with the pre-determined ITI

sequences. We expected that participant performance would demonstrate entrainment to the sinusoids in the neighborhood of the frequency of the input signal. The oscillating pattern is only slightly less predictable than a fixed ITI version of the task, such that the timing of recent trials will be similar to an upcoming trial. On the other hand, the fixed and sinusoidal ITIs are both more predictable than randomly presented ITIs. We hypothesized that participants would express weaker coordinative activity in the random ITI condition (e.g., see Holden et al., 2011; Van Orden et al., 2003). In line with previous temporal estimation studies, we predicted the ITI manipulation would yield little to no impact on the key-press duration series (Holden et al., 2011).

## **2.1 Method**

### **2.1.1 Participants**

Fifty introductory psychology students participated voluntarily as one of several paths to fulfilling an outside-of-class research requirement. Ten students were randomly assigned to each of the five conditions: constant, random, HF, LF, or BF ITI. All data collection and retention practices for Experiments 1, 2, & 3 were IRB approved and informed consent was obtained using an information-sheet consent procedure.

### **2.1.2 Apparatus**

A standard PC controlled signal presentations and data collection. The sine wave manipulations varied the range of durations of the blank-screen presented in between the offset of the ready signal and the onset of a signal to respond. The vertical raster-refresh cycle of the video monitor was 72 Hz. A video-controller refresh-cycle freezing routine allowed the blank screen durations to be controlled to the nearest millisecond (Bührer, Sparrer, & Weitkumat, 1987). The ready signal and signal to respond were presented in the center of the video monitor. A 6ms allowance was incorporated into the reported display durations, the time required for the raster to pass the center of the display during its refresh cycle.

### **2.1.3 Procedure**

Participants were instructed to respond by pressing a joystick trigger-button once they determined the visual stimulus (i.e., #####) had been displayed on the screen for 700ms. Participants responded by pressing the primary trigger button of a standard four-button joystick with their index finger. The direct input (non-buffered) joystick was positioned directly in front of the participant's dominant hand and recorded the temporal interval to the nearest millisecond. Temporal intervals were measured from the onset of the signal. Participants typically completed the 64 introductory trials within approximately three minutes, and the 1,100 trials within approximately 20 minutes. In addition, we collected successive key-press intervals. A key-press duration is the interval of time that elapses from the key-contact, that determines the temporal estimate, until the subsequent key-release response breaks circuit contact (compare Kello et al., 2007; Holden et al., 2011). Key-press durations about each response time, indicating the button-release dynamics unfolding at the onset of each ITI.

Participants were randomly assigned to one of five conditions, which varied the rate at which stimuli were presented. For the baseline condition, each trial began with a signal to respond (#####) displayed in the center of a computer monitor. Following a button-press response, the blank screen was maintained for a constant ITI of 700ms, after which, a constant delay of 418ms was added to the blank screen interval and was then replaced by a new signal to respond. The signal to respond remained visible until a

response was recorded, or for a maximum of 5004ms.

Four additional conditions varied the presentation duration of the ITI, or the blank screen between the response and the onset of the next stimulus. Three ITI conditions introduced a sinusoidal pattern of changes to the ITIs and one condition was comprised of a randomly shuffled version of the summed sinusoids. The sinusoidal manipulations altered the ITI length and frequency of oscillation. The first sinusoidal condition introduced a high-frequency (HF) oscillation that completed a cycle every 8 trials (i.e., an 8-trial period). This rate of oscillation corresponded to a frequency of .125 for the 127-frequency spectral analysis that is used to test for  $1/f$  scaling. The low-frequency (LF) wave completed a cycle every 20 trials (i.e., a 20-trial period) and had a frequency of .051 in the power spectral analysis. The two specific sinusoids were chosen because they do not share common harmonics and correspond to frequencies estimated by the spectral analysis routine. A third sinusoidal condition summed the slow and fast frequency waves from the first two conditions in order to derive a sine wave that varied along both frequencies (BF). The ITIs from the summed sine condition were randomized to yield a second baseline condition of random ITIs. The randomized ITIs were subsequently presented in the same fixed order to all participants in the random cell. The constant and randomized ITI conditions served as control conditions for use in statistical contrasts with the sinusoidal conditions. The mean duration of all variable ITIs was always 700ms, and the standard deviation of all variable ITIs was 180ms.

#### **2.1.4 Analyses**

A fractal pattern of variation is often portrayed using spectral analysis of repeated measurements. Repeated measurements can be characterized by the size of changes across measured values and the frequency of changes of a particular size, or how often changes of a particular size occur. The fractal pattern relates amplitude and frequency of variation in a power-law scaling relation. The scaling relation between the size of changes, and how often changes of that size occur, is inversely proportional on logarithmic scales. As shown in Figure 1, the amplitudes of variation can be seen to scale with frequency of variation such that  $S(f) \propto f^{-94}$ . The present studies used scaling exponents as a dependent measure of stochastic synchronization across timescales. Larger scaling exponents indicate a more robust pattern of scale-free coordination. Scaling exponents that are statistically equal to zero indicate the absence of scale-free coordinative activity. Figure 1 illustrates the statistical basis for spectral scaling exponents. Holden (2005) provides a detailed tutorial on the spectral analysis of response time trial-series.

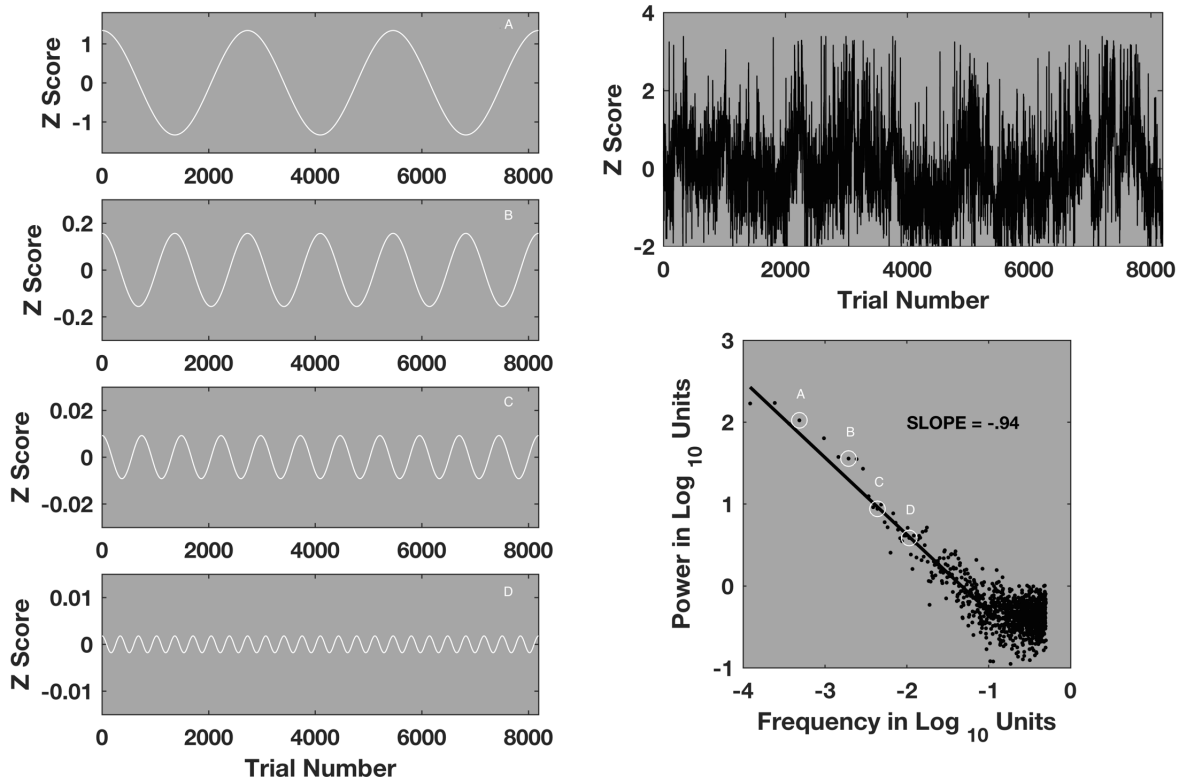


**Figure 1. Scaling exponent of reaction-time trial-series.** The left panel of plots illustrates several component frequency bands that can be extracted from a typical reaction-time trial-series. The trial-series depicted in the upper right plot reflects the variation typical of within-participant response times, including slow and fast timescale changes. Individual frequency bands can be extracted and plotted based on their frequency and amplitude of fluctuation (left panel, Plots A, B, C, & D). The specific depicted frequencies span 3 orders of amplitude and correspond to the lettered and circled coefficients depicted in the spectral scatter plot on the lower right corner of the figure. The Y-axis of the spectral portrait in the lower right plot corresponds to amplitude of fluctuations, or size of change, and its X-axis refers to their frequency of occurrence, on log-log scales. Since  $f^{-\alpha} = 1/f^{\alpha}$ , the size of change,  $S(f)$ , is proportional to the frequency,  $f$ , of change, as  $S(f) \approx 1/f$ . The scaling exponent,  $\alpha$ , relates amplitude and frequency of variation and is depicted as  $\alpha = .94$ . The scaling exponent is derived from the regression slope of the spectral coefficients in lower right plot. The scaling exponent characterizes the relative coherence of a scaling relationship across the timescales of measurement (Response time data from Van Orden, et al., 2005).

Fourier-based wavelet analyses are closely related to spectral analyses, but, unlike spectral analysis, wavelet techniques preserve temporal information about a signal's fluctuations. As the name implies, a wavelet is a discrete wave-like function that is systematically shifted and rescaled to capture time-series variability (Percival, & Walden, 2006). This feature allows the relative amplitude of each frequency to be estimated across the successive observations in a time series. Wavelets can therefore be used to create band-pass filters to extract variability only at the specific frequencies of the sinusoidal inputs. The resulting reconstructed time-series are smooth and

differentiable. As such, they meet the requirements for the application of phase-space reconstruction and cross-recurrence analysis.

Wavelet-then-cross-recurrence analyses quantifies the coupling or attractor strength ( $|\lambda|$ ) between two oscillatory patterns as well as the relative influence of external perturbations ( $Q$  and  $SD\Phi$ , Pellicchia, Shockley, & Turvey, 2005; Richardson, Schmidt, & Kay, 2007, see Figure 2 tutorial). This procedure was used in the present study to identify relationships between the input sinusoids and performance variability at the same frequencies. These analyses determined the extent to which attraction to a common phase and frequency is sufficient to explain coordination with the driving force provided by the manipulation.

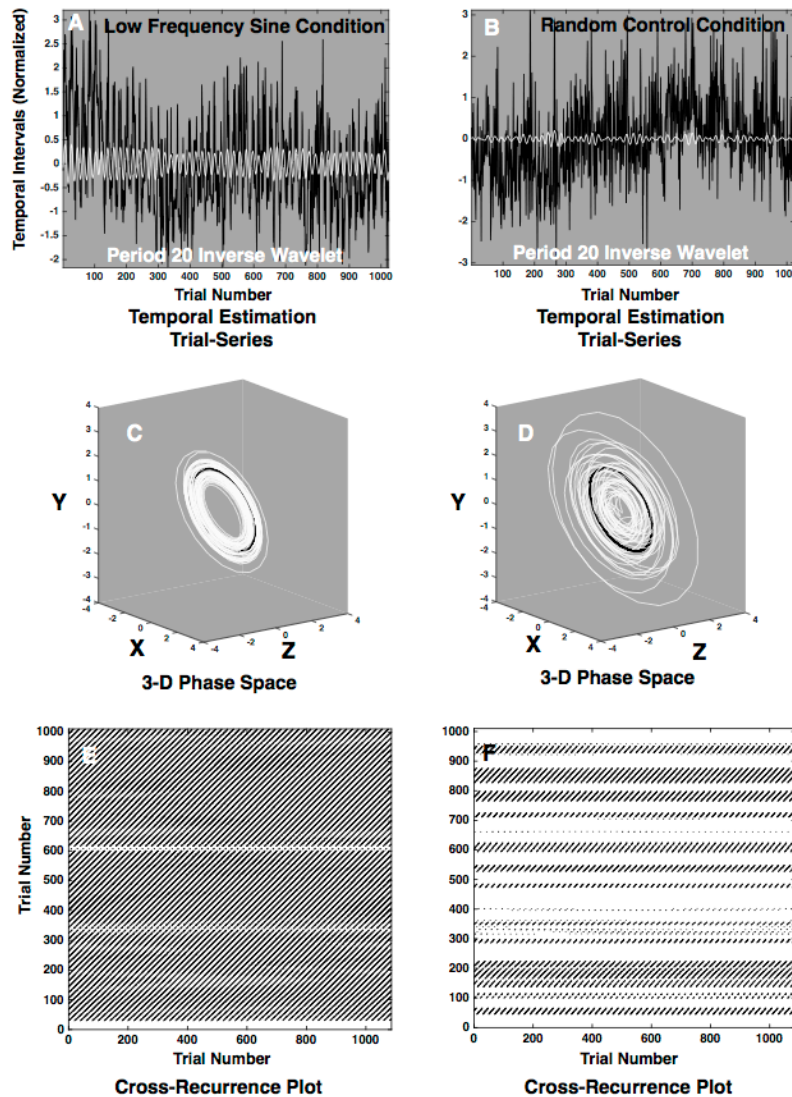


**Figure 2. Quantifying dynamic attraction between an input sinusoid and temporal estimation time-series.** *The black line in plot A depicts a typical temporal estimation trial-series from the LF period-20 sinusoidal ITI condition. By contrast, the black line in plot B illustrates a typical temporal estimation trial-series from random ITI control condition. The Fourier-based wavelet analysis was used as a band-pass filter to isolate trial-series variability at the same frequency as the LF period-20 sinusoidal ITI for both trial-series. The white lines in both plots A and B depict the resulting frequency-*

*isolated time-series that were reconstructed through an inverse-wavelet operation from each respective empirical trial-series. In plot A, the frequency isolated time-series displays large-amplitude oscillations with the same period as the ITI signal. This pattern is maintained throughout the sinusoidal experimental session—behavior that is symptomatic of entrainment. The signal reconstructed from the random ITI control series, and depicted as a white line in plot B, illustrates the absence of entrainment. Here, the oscillations are transient and maintain relatively low inconsistent amplitudes over time. In the center row, plots C and D, depict the result of a phase-space reconstruction on both inverse wavelet signals. Plots C and D depict the LF ITI input series as a black circular line embedded in the center of more variable three-dimensional phase-space plots of the inverse-wavelet signals, depicted as white lines. Plot C illustrates relatively coherent, and tight coordination between the LF ITI and empirical sinusoid derived from participants in the LF condition. On the other hand, plot D illustrates loose and wobbly phase relationships between the ITI and empirical sinusoid derived from participants in the random condition. This is again symptomatic of the absence of coherent coordination. Finally, the two bottom plots (E and F) depict cross-recurrence plots that were used to quantify the relative coordination between an ITI input sinusoid and a band-pass wavelet signal, derived from the empirical time-series. Synchronized trajectories appear as coherent and evenly spaced diagonal lines (Plot E), while incoherent trajectories result in either no texture, or patterns other than relatively continuous diagonally oriented lines (Plot F). Thus, the sine manipulation in plot E indicates strong and persistent coordination, and the random control manipulation in plot F indicates weak and unsystematic coordination. The attractor strength ( $\lambda$ ) and noise amplitude ( $Q$ ) statistics, described in the text, are computed from measures derived from the texture of the recurrence plots. Between-group statistical contrasts compared the ITI sinusoids to inverse-wavelets, PSR, and cross-recurrence plots that were computed on empirical series from both the constant and random ITI conditions. This procedure yielded empirically derived baseline signals that are representative of transient and chance-level coordination. ITI = Inter-trial Interval, HF = High Frequency, LF = Low Frequency, BF = Both Frequencies PSR = Phase space reconstruction.*

The phase-space reconstruction (PSR) analysis uses four time-delayed copies of the one-dimensional frequency-isolated time-series to “embed” the frequency-isolated time-series into a surrogate multi-dimensional phase-space (see Abarbanel, 1996). The surrogate phase space reveals and relates position information to higher derivatives of change across time. The PSR plots in Figure 2 depict example three-dimensional phase spaces. The present analyses used a four-dimensional embedding space, a time-delay equal to  $\frac{1}{4}$  of the input sinusoid’s period, or their integer average for the BF condition (low = five trials, high = two trials, both = four trials). A constant 0.7 standard deviation (SD) was used as a recurrence radius for all experiments, conditions, and analyses. This radius was selected because it returned the percent recurrence values for all studies in the recommended neighborhood of 1% to 5% for these analyses. The same parameters used for a given sinusoidal condition were then applied to the constant and random conditions to generate baselines for our statistical contrasts.

Finally, cross-correlation analyses were used to directly evaluate alternative hypotheses that posit short-range lagged correlations with the ITI series as the basis for any synchronization with the sinusoidal ITI series. A cross-correlation analysis computes the linear association between two signals at various temporal leads and lags in the form a Pearson correlation coefficient. In this case it was used to determine the strength of association between each sinusoidal input signal and the matrix of participant’s temporal estimation and simple reaction time series.

## 2.2 Results

The following analyses tested for and characterized different aspects of entrainment in temporal estimation performances across the ITI conditions. First, standard spectral analyses were conducted to compare the patterns of mono-fractal  $1/f$

scaling across the five conditions. This analysis examined the presence of coordination near the frequency of the input sinusoid (Holden, 2005; Press, Teukolsky, Vetterline, & Flannery, 1992) and determined if the input sine reliably affected other timescales of change. The second set of analyses began with continuous Fourier-based wavelet analyses (Torrence & Compo, 1998). The wavelet analyses approximated a band-pass filter to isolate and extract performance variability at the same frequency as the sinusoidal inputs. Next, phase-space reconstruction and cross-recurrence analyses were conducted to identify the relative strength of the coupling between the participant's temporal estimation series and the sinusoidal manipulations. Finally, cross-correlations were used to quantify the empirical and ITI phase relations and evaluate an alternative hypothesis that simple short-range, -1 lag associations with the ITI signals are the basis of any observed coordination.

### 2.2.1 Spectral analyses

As a first step for the spectral analyses, temporal estimates less than 10ms or greater than 5 s were eliminated from each trial-series. Observations that fell beyond  $\pm 3$  standard deviations from the series mean were eliminated, and the series were then normalized. Next, a window-averaged 127-frequency power spectral density was computed for each series (Holden, 2005). The spectral power coefficients derived at each frequency were then averaged with those of the same frequency, across all ten participants in each of the five conditions. This yielded an aggregate power spectrum for each condition. Key-press durations have a more limited range of variability than temporal estimates and did not require absolute censoring. However, key-press durations greater than 3 *SD* from the participant's mean key-press duration were eliminated for the purposes of the spectral analysis.

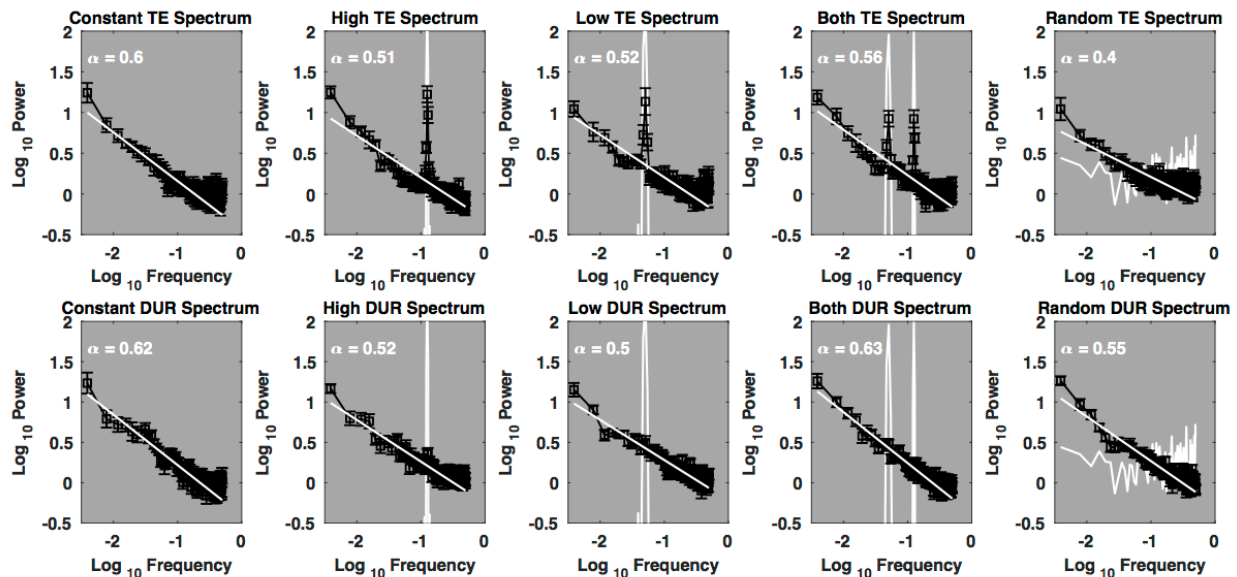


**Figure 3. Temporal estimation and key-press duration power spectra.** *The black error bar plots in each panel depict the aggregate temporal estimation (top row) and key-press duration (bottom row) power spectra for the constant, sinusoidal and randomized ITI conditions. The temporal estimation spectral analyses revealed reliable sinusoidal entrainment at the same frequency as the input oscillation, plotted as vertical white lines, that was robust enough to penetrate the broadband 1/f scaling. By contrast, the key-press durations were not notably influenced by the sine manipulations. The power spectrum of the randomized ITIs is depicted as a jagged horizontal white line on the far-right plots, that is*

*symptomatic of white noise.*

The upper leftmost plot of Figure 3 depicts the aggregate spectral portrait of the baseline temporal estimation condition. The spectral plots illustrate the mean amplitude of each estimated frequency and the error bars represent one standard error of the mean. The fixed ITI plot reveals a power spectrum that is representative of standard computer-paced temporal estimation performance. The overall shape of the power spectrum is consistent with a  $1/f$  scaling relation (e.g., Gilden, 2001; 2009; Holden, 2005). A standard log-log regression, computed using the coefficients of the lowest 50% of the frequencies yielded scaling exponents ranging from  $\alpha = .51$  to  $.60$  for the control and sinusoid cells, and  $\alpha = .38$  for the random cell. Except for the spectral spikes at the input frequencies, the trial-series across conditions yielded power spectra consistent with fractal scaling. The presence of scaling was confirmed by a series of off-line statistical tests that are not reported for space considerations (i.e., 512-trial spectra and shuffling tests, see Holden, Van Orden, & Turvey, 2009, p. 329, and  $t$ -tests contrasting the distance of spike heights from the  $1/f$  scaling line).

The bottom five spectral plots in Figure 3, of the key-press duration (DUR) series, did not reveal a reliable influence of the five ITI manipulations. The average scaling exponent of the key-press intervals remained relatively constant across the five conditions, ranging from a minimum of  $\alpha = .50$  to a maximum of  $.62$ . The spectral plot of the HF DUR condition in Figure 3 hints at an influence of the ITI sinusoid, but, if present, the influence is marginal. Overall, visual inspection of the averaged intact spectra establishes a linear scaling on double logarithmic axes, and, in conjunction with the outcome of (unreported) random shuffling tests, was consistent with  $1/f$  scaling.

The influence of the sinusoidal ITI manipulations on the time series of temporal estimates are represented as averaged power spectra of three sine wave conditions in Figure 3. The three plots in the center of the upper row of plots depict the temporal estimation power spectra for the high, low, and high-plus-low ITI waves. All three power-spectra are sloped in a manner consistent with  $1/f$  scaling. The spectral exponents of these three plots remain relatively unchanged from that of the baseline condition ( $\alpha = .60$ ). The average spectral exponents of the sine conditions are  $\alpha = .51$ ,  $.52$ , and  $.56$  respectively. The impact of the sinusoidal oscillations in the ITIs can be clearly seen as a “spike” in the spectral plot corresponding to frequencies of the ITI manipulation. Again, off-line  $t$ -tests indicated the spikes reliably exceeded the amplitudes predicted by the scaling relation itself. In this case, the impact of the sine ITI manipulations appears to be largely additive with the  $1/f$  scaling.

The next step was to characterize the influence of the manipulation on performance in terms of attractor dynamics. The *Analyses* section describes a number of statistical tools designed to assess the patterns of interaction among coupled oscillators. Figure 2 is a brief visual tutorial of each signal processing procedure required to derive estimates of attractor strength and noise amplitude. In addition, the associated citations refer readers to more detailed treatments of each step in the statistical analyses examining attractor dynamics. Next, a series of analyses characterizes the relative strength and nature of the attraction or coupling between the oscillations embedded in the ITIs and each participants' time-series of temporal estimates.

### 2.2.2 Attractor strength and noise amplitude

Recurrence analyses were used to compute two dynamical indicators: *attractor strength* ( $\lambda$ ) and *noise amplitude* ( $Q$ ). Attractor strength was estimated by computing a near-equilibrium Lyapunov exponent, or lambda ( $\lambda$ , Richardson, et al., 2007). Lambda quantifies the rate at which a perturbed oscillator re-synchronizes to a driving sinusoidal pattern, such as the oscillating ITIs. A related  $Q$  statistic estimated the overall strength of the stochastic noise that is present in the system. Entrainment dampens dynamic noise, such that relatively lower  $Q$  values are symptomatic of more robust coordination. Cross-recurrence analysis (Zbilut, Giuliani, & Webber, 1998) was used to compute  $\lambda$  with respect to the input sinusoid for each of the three conditions used that included a sine manipulation. Variability at the same frequencies was extracted from the constant and random ITI conditions, and  $\lambda$  and  $Q$  were computed to serve as baseline estimates in statistical comparisons.

Next, analyses were directed at examining influence of the sinusoidal ITIs, over and above the inherent patterns of oscillation entailed in  $1/f$  signals and other intrinsic sources of variability. Since there was no clear a-priori way to decide if the statistics derived from either the constant or the random ITI cells might yield larger or smaller average  $\lambda$  and  $Q$ , each statistical test combined the values from both control conditions into a single aggregate 20-participant control group. By contrast, the sinusoidal cells always contained data from ten participants. This contrast allowed for the extraction and reconstruction of baseline variability at the same frequencies as the sine manipulations, all from performances in which entrainment was known to be absent. Identical statistical operations and parameters were applied to control group and sinusoidal data sets in order to draw equivalent entrainment comparisons.

A one-way between-subjects analysis of variance (ANOVA) that contrasted the ten lambda ( $\lambda$ ) values from the HF (period 8) condition with the 20 lambda values derived from the combined control group revealed reliably larger average lambda values in the period 8 sine ITI condition,  $F(1, 27) = 14.04$ ,  $r^2 = .34$ ,  $p < .05$ , ( $M_{HF} = .06$ ,  $SD = .04$ ;  $M_{Control} = .03$ ,  $SD = .01$ ). The same analysis, conducted on the LF ITIs (period 20) also revealed reliably larger lambda values as compared to the control group,  $F(1, 27) = 11.58$ ,  $r^2 = .30$ ,  $p < .05$ , ( $M_{LF} = .12$ ,  $SD = .09$ ;  $M_{Control} = .06$ ,  $SD = .02$ ). Likewise, the group exposed to both frequencies (Period 8 & 20) yielded reliably larger  $\lambda$  values than controls,  $F(1, 27) = 18.05$ ,  $r^2 = .39$ ,  $p < .05$ , ( $M_{BF} = .03$ ,  $SD = .009$ ;  $M_{Control} = .016$ ,  $SD = .004$ ). The sinusoidal patterns acted as attractors and entrained temporal estimation performance across all three sinusoidal ITI conditions. The key-press duration series were submitted to the identical statistical analyses and no reliable coupling between the ITI sinusoids and the key-press durations were detected (all  $F$ 's  $< 1$ ).

The same one-way between-subjects ANOVA design was used to contrast the ten  $Q$  values from the HF ITIs (period 8) condition with the 20  $Q$  estimates derived from the combined control group. It revealed reliably smaller average  $Q$  values in the period 8 sine ITI condition than the control group,  $F(1, 27) = 5.13$ ,  $r^2 = .16$ ,  $p < .05$ , ( $M_{HF} = 27.11$ ,  $SD = 16.52$ ;  $M_{Control} = 36.88$ ,  $SD = 6.86$ ). The same analysis, contrasting the LF ITI (period 20) condition with controls also revealed reliably smaller  $Q$  values in the LF condition as compared to the control group,  $F(1, 27) = 23.84$ ,  $r^2 = .46$ ,  $p < .05$ , ( $M_{LF} = 21.18$ ,  $SD = 6.75$ ;  $M_{Control} = 37.11$ ,  $SD = 9.2$ ). Similarly, the group exposed to both frequencies (Period 8 & 20) yielded reliably lower  $Q$  values than controls,  $F(1, 27) =$

9.30,  $r^2 = .25$ ,  $p < .05$ , ( $M_{BF} = 210.47$ ,  $SD = 67.5$ ;  $M_{Control} = 309.65$ ,  $SD = 90.78$ ). Overall, the sinusoidal manipulations were associated with a reduction in the magnitude of stochastic noise entailed in temporal estimation, at the input sine frequencies, as estimated by cross-recurrence analysis. Just as with the  $\lambda$  analysis, contrasts of the Q statistic on the key-press duration series failed to reveal a reliable change in the magnitude of stochastic noise at the frequency of the ITI sinusoids (all  $F$ 's  $< 1$ ).

#### **2.2.4 Entrainment alternatives**

One might propose an alternative short-term autocorrelation explanation for the observed patterns of entrainment in temporal estimation performance, consistent with weak anticipation. For instance, post-hoc cross-correlation analyses revealed the maximum correlation with the ITI series was nearly always the immediately prior trial (a -1 lag, see Figure 4). The cross-correlation function of two sine functions is itself a sine function. As such, the sine condition cross-correlation functions returned sinusoids with -1 lag maxima. The dominant relative phase relationship between temporal estimation trial-series and the sinusoidal ITI signals was anti-phase, as demonstrated by negative sign of the reliable -1 lag correlations in the sine conditions.

Perhaps the most compelling indication that short-range autocorrelation supported temporal estimation performance came from the random condition. By contrast to the oscillating pattern of statistical significance observed in the sine cross-correlation functions, only the -1 lag of -.34 achieved statistical significance in the random condition. We used this parameter, in conjunction with synthetic  $1/f$  scaling, to implement an autoregressive (AR) model of the temporal estimation trial-series. The goal was to determine what aspects of the empirical patterns could be accounted for by a simple short-range -1 lag AR model that approximates the behavior of short-term perceptual stores.

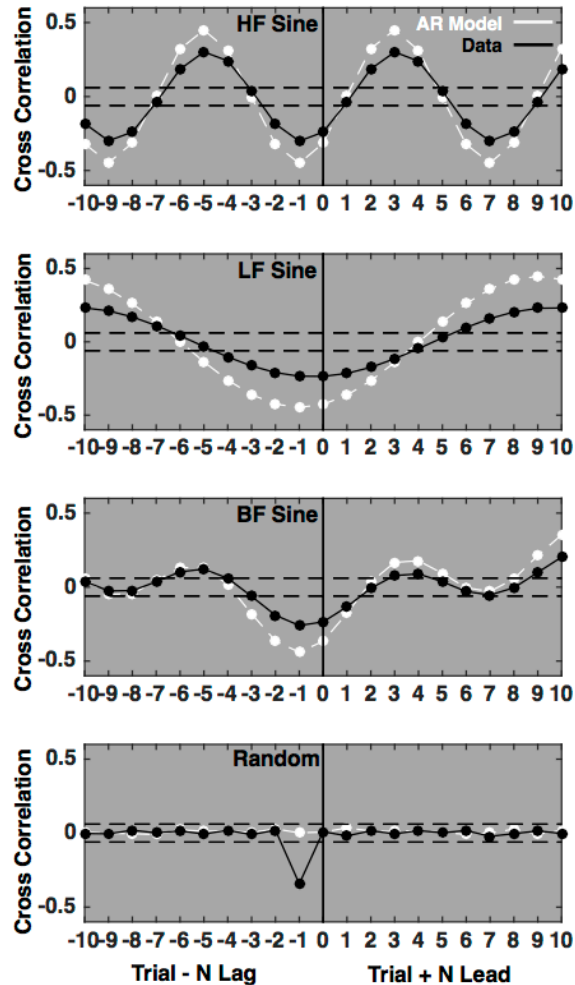


**Figure 4. Cross-correlations of empirical data and autoregressive model.** Empirical cross-correlations functions are depicted in black for the HF, LF, and BF ITI conditions, as well as the random ITI condition. Reliable positive lags indicate anticipatory associations with the ITI signals, reliable negative lags indicate historical associations with the respective ITIs, and a reliable lag-zero indicates an instantaneous association with an ITI series. The white lines in each plot depict the cross-correlation functions for an autoregressive (AR) model that illustrates the expected performance profile if a -1 lag of the ITI values govern participant's temporal estimates. The model for all conditions used the -1 lag correlation of -.34 observed in the random ITI condition as the AR parameter. The -1 lag for the random condition was the largest among the different conditions. While the large AR coefficient might explain the model's overshoot in the sine conditions, it does not explain why the AR model failed to approximate the -1 lag association in the random condition from which it was derived. The solid vertical lines in the middle of each plot indicate a zero lag, in which the collected response on the trial was to the presented ITI. The dashed horizontal lines indicate the cutoff for statistical reliability,  $r = .06$  ( $\pm 2/\sqrt{1090}$ ) that was used for all cross-correlations. No data censoring procedures were used so that phase relations would be preserved. Detrending all the trial-series prior to the analysis yielded identical cross-correlation outcomes. Identical simulation outcomes resulted when the fractal scaling was synthesized from the temporal estimation time-series themselves, using an iterated amplitude adjusted Fourier transform algorithm (Schreiber & Schmitz, 1996). ITI = Inter-trial Interval, HF = High frequency, LF = Low frequency, BF = Both frequencies.

A -1 lag model comprised of a weighted sum of 34% negative correlation with the prior ITI and 66%  $1/f$  scaling captured the bulk of the qualitative variability in the

sinusoidal conditions. This outcome paralleled a report in the context of a synchronized tapping task (Torre et al., 2013). Their tapping study was designed to discriminate synchronization through global behavioral tuning, sometimes called *strong anticipation* (e.g., Stepp & Turvey, 2010), from *weak anticipation*, in which performance relies on local error corrections derived from the previous trial. Torre et al. (2013) found that simple autocorrelation error corrections based on the previous (-1 lag) inter-tap and ISIs successfully approximated synchronized tapping to metronome signals that included long-range, short-range, random, and even short-term anti-persistent but long-range persistent signals.

Along these lines, the -1 lag ITI correlation plus  $1/f$  scaling AR model mostly succeeded in reproducing the aggregate sinusoidal patterns. However, this model failed to approximate the random condition data from which its own parameters were derived. That is, the empirical random ITI data expressed a clear -1 lag—it was used to parameterize the -1 lag model simulations. However, none of the cross-correlations in the simulated random condition were reliable. Furthermore, the lagged correlation with the random ITI failed to weaken or *whiten* the  $1/f$  scaling of the simulated series enough to agree with the empirical random condition: an 8% scaling-exponent reduction in the simulations versus a 37% reduction in the performance data.

Nevertheless, if -1 lag correlation models can do so much work, then why invoke synchronization among coupled oscillators? In fact, autocorrelation, cross-correlation, and spectral analysis are mathematically very similar. However, they differ in that simple correlations establish associations but offer no intrinsic scientific motivation for the relationships they identify. The explanatory role of the entrainment hypothesis is supported by its success in related experimental domains, such as human movement science, and other biological and physical systems (e.g., Kugler & Turvey, 1987; Strogatz, 2003).

It is well-established that oscillators with more similar intrinsic frequencies are likely to express more robust entrainment than comparable oscillators with dissimilar intrinsic frequencies. The frequency difference between two oscillators is indexed by a detuning parameter ( $\Delta\omega$ ) and is relevant to equations that describe the coupling strength of oscillators. If oscillatory entrainment supports coordination with the ITI sine, then the strongest relative coupling strength should be for participants with mean temporal estimates closest to the 700ms period of both pure sine ITIs. By contrast, coordination should be weaker for participants with average temporal estimates far from the 700ms target value. This amounts to a prediction of an inverted quadratic relationship between the participants' mean temporal estimates and their relative detuning levels. The  $SD\phi$  statistic approximates a detuning parameter with measures of coordination variability. It is derived from the cross-recurrence based estimates of  $\lambda$  and  $Q$ , as follows (see Richardson, et al., 2007):

$$SD\phi = \sqrt{\frac{1/prop\%REC}{2*propL_{max}}} \quad (1)$$

The left panel in Figure 5 depicts this statistically reliable quadratic relationship,  $F(2,17) = 8.29$ ,  $r^2 = .49$ ,  $p < .05$ . Participants that generated temporal intervals near the targeted 700ms interval displayed enhanced entrainment relative to participants that typically produced intervals that drifted further from their 700ms target (white circles in left plot of Figure 5).

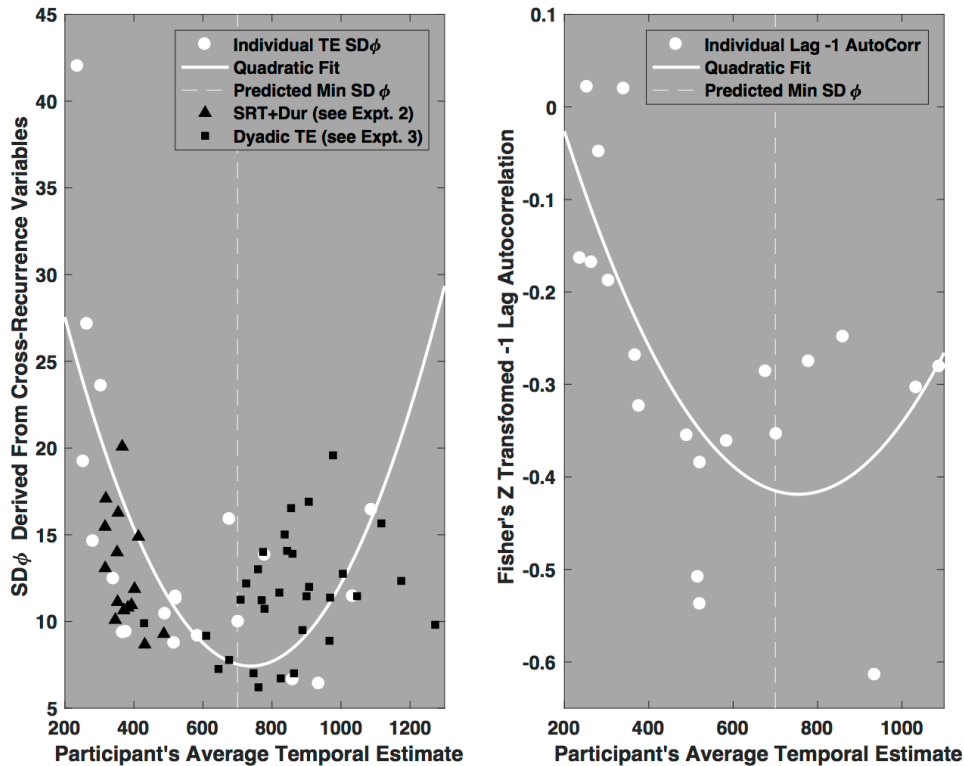


**Figure 5. Frequency detuning relationship between temporal estimation and sinusoidal manipulation.** The X-axis on both plots depicts the mean temporal estimate for each of the participants in the high and low frequency sinusoid conditions as open white circles. Both HF and LF sinusoids used the same 700ms average duration, indicated by the vertical dashed white line. The Y-axis on the left plots depicts a measure of relative phase variability, based on the cross-recurrence statistics. Roughly speaking, relatively lower values indicate more stable entrainment than relatively larger values. The white curve depicts a least squares quadratic fit to the white circles and illustrates the reliable inverted-U shape predicted by frequency detuning. The white circles represent the mean temporal estimates of Experiment 1 participants assigned to the sinusoid conditions. The black triangles depict the  $SD\phi$  values for a sum of the LF reaction times and key-press durations of Experiment 2. They comply with the temporal estimation detuning relationship and are discussed in the Experiment 2 Results section. Likewise, the black squares depict the results of the  $SD\phi$  analysis on the dyadic temporal estimation task. The dyadic performances were also consistent with the detuning prediction and are discussed in the Experiment 3 Results section. The X-axis on the left plot depicts participant's -1 lag correlation with the ITI signals. Their association strengths are also consistent with the detuning hypothesis. Apparently, the lagged correlations are sensitive to the frequency detuning that is characteristic of oscillatory entrainment. However, short-range regression (ARMA) models do not anticipate frequency detuning. LF = Low frequency, ITI = Inter-trial-interval. ARMA = Auto-regressive-moving-average.

The right plot in Figure 5 lends additional support for synchronization dynamics as the basis of the observed -1 lag autocorrelations. It depicts the strength of each individual participant's Fisher's-Z transformed -1 lag correlation ( $r$ ) with the HF and LF ITI sinusoids as white circles. The strength of these associations is mediated by the

average duration of the participant's temporal intervals. The relationship follows the same quadratic detuning pattern predicted from the synchronization hypothesis,  $F(2,17) = 7.91$ ,  $r^2 = .48$ ,  $p < .05$ . The -1 lag correlations are strongest in the neighborhood of the 700ms average period of the sinusoids.

In this case, the lagged correlations are proxies for measures of coordinative dynamics. For example, multiple and semi-partial regression analyses, using participant's average temporal estimates as a dependent variable indicated that  $SD\Phi$  and the Fisher's -1 lag  $r$  share 37% of the variance in the mean temporal estimates, and neither variable reliably explains more variance than the other. The  $SD\Phi$  and the Fisher's transformed  $r$  are mathematically redundant, but they are theoretically distinct. The mathematics of synchronization offer a principled explanation for the observed frequency detuning, while the mathematics of regression simply indicate the presence of an association. ARMA models have the capacity to provide reasonable descriptions of these performances, but they are necessarily agnostic with regard the explanatory basis for the observed coordination (also see, Gilden, 2009).

In sum, participant's temporal estimation performances entrained to the sinusoidal test signals. Moreover, performance conformed to the expected behavior of standard dynamical attractors. As attraction strength ( $\lambda$ ) increased, stochastic noise ( $Q$ ) decreased, such that the sinusoids stabilized and entrained our participant's performances.

### 2.3 Discussion

The aggregate spectral analyses identified the presence of amplitude spikes in frequencies that corresponded to the sinusoidal manipulations, signaling increased power over and above the stochastic coordination indicated by  $1/f$  scaling in temporal estimation performance. Spectral and cross-recurrence analyses captured the impact of the sinusoidal manipulations, indicating that participant's temporal estimation performance became entrained to the sinusoidal ITI input. By contrast, spectral and cross-recurrence analyses revealed that the key-press duration series did not become entrained to the sinusoidal ITI manipulations. Temporal estimation emphasizes the repeated production of identical time intervals. Overall, the participants expressed an anti-phase coupling with the sinusoidal fluctuations unfolding in the downtime between trials. Entrainment to the sinusoidal manipulation implicates this time-keeping activity as a fundamentally dynamic activity that is supported by synchronization principles (Balasubramaniam, 2006; Schöner, 2002; Torre, et al., 2013).

A frequency detuning analysis established oscillatory entrainment as the basis of the observed coordination. The -1 lag correlation hypothesis failed to explain the clear detuning pattern. Weak anticipation error-corrections are based on the duration of preceding signals to respond, and/or the preceding responses themselves.

Autoregressive-moving-average (ARMA) model parameters controlling correlation magnitude are assumed to vary unsystematically across participants. Similarly, the mean duration of temporal estimates is assumed to vary unsystematically across subjects and is either removed through normalization or treated as free constant in modeling enterprises. Lagged error-correction and ARMA models simply do not anticipate systematic variation in coupling strength based on frequency detuning. The entrainment hypothesis captured more detail in the empirical patterns, such that the principles governing oscillator dynamics carried a heavier theoretical load than the

case-by-case hypothesis of  $-N$  lagged association.

When regular oscillations were introduced in a narrow frequency band, only those frequencies were strongly affected. This suggests the ongoing coordinative activity supporting performance is flexible enough to capture, accommodate, and exploit this source of environmental regularity. Entrainment to the embedded oscillatory manipulations was superposed on a background of  $1/f$  scaling. By contrast, the very low amplitude, randomly changing ITIs in the random condition influenced entire  $1/f$  scaling relations by uniformly weakening them (Holden et al., 2011). There is little long-term regularity to be exploited in randomized ITI sequences. Presenting the ITIs in an unsystematic sequence perturbed the broadband coordinative structures that support performance, disturbing patterns of coordination typically observed during tasks with constant or oscillating ITIs. The context of the coordination observed in the sinusoidal signals suggests the whitening in the random condition results from participant's attempts to coordinate with the random ITI signal.

More generally, the successful entrainment manipulation illustrates that cognitive activities are capable of systematically coordinating with constraints supplied by the context of the immediate environment, even on timescales much slower than those presumably occupied by the specified cognitive act (Sreekumar, Dennis, Doxas, 2016; Sreekumar, Dennis, Doxas, Zhuang, & Belkin, 2014; Van Orden, et al., 2012; Wijnants, et al., 2009; 2012). In this case, the slowly oscillating across-trial ITI durations constrained the much faster timescale, within-trial temporal estimation performances. The findings illustrate how this coordinative activity could be straightforwardly characterized and quantified in terms of established properties of oscillatory dynamics. Dynamic coupling to task and environment appears to be an inherent property of this behavioral system. Next, we imbed identical oscillatory patterns in the inter-stimulus-intervals of a simple reaction time task.

### **3. Experiment 2: Sinusoidal synchronization in simple reaction time**

Temporal estimation emphasizes timescales slower than the pace of individual trials, because the task requires participants to make their successive temporal interval judgments as similar as possible across trials. Next, we introduce the sinusoidal fluctuations to the inter-stimulus-intervals (ISIs): the elapsed time between the presentation of a fixation stimulus (+++) and a response target (#####), in a simple reaction task. By contrast to the temporal estimation task, a simple reaction task requires participants to respond quickly and accurately with a predetermined response to the response target during each trial. The typical time course of a simple reaction time performance is in the neighborhood of 200 to 300ms, which is much faster than the 700ms average duration of the sinusoids. Therefore, a simple reaction time protocol imposes task requirements that emphasize faster timescales of cognition and action than a temporal estimation protocol.

Speeded responding reduces variability in successive response time trials, relative to temporal estimation. An entrainment perspective suggests that a simple reaction time task will yield weaker coupling to ISI changes, as compared to the temporal estimation ITI changes. Alternatively, the  $-1$  lag correlation model prescribed by the weak anticipation hypothesis predicts qualitative outcomes identical to those observed in the aforementioned temporal estimation and synchronized tapping cross-correlation analyses (Experiment 1; Torre et al., 2013). That is,  $-1$  lag models do not

address the distinct task demands, predicting that any observed sinusoidal coordination is governed by the ISI presented on the previous trial, just as for temporal estimation.

### **3.1 Method**

#### **3.1.1 Participants**

Seventy-five introductory psychology students participated voluntarily as one of several paths to fulfilling an outside-of-class research requirement. Fifteen students were randomly assigned to each of five ISI conditions: constant, random, HF, LF, or BF.

#### **3.1.2 Procedure**

The ISI manipulations were identical to those used for the ITI manipulations in Experiment 1. Each trial began with a ready signal (+++) displayed in the center of a computer monitor. The ready signal was visible for 171ms and then replaced by a blank screen. The ISIs were inserted in the downtime between the offset of the ready signal and the onset of the signal to respond (#####, displayed in the center of the computer monitor). Participants were instructed to respond as quickly as possible after the presentation of the signal to respond by pressing a joystick button with their index finger. The non-buffered joystick was positioned directly in front of the participant's dominant hand, and recorded response time to the nearest ms from the onset of the signal. In addition, the software recorded the duration of each key-press. The time interval from each response until the next ready signal was 418ms. Participants completed the 64 introductory trials within about three minutes and the remaining 1,100 experimental trials within approximately 20 minutes. Introductory and experimental trials were otherwise identical.

### **3.2 Results**

We conducted the same series of statistical analyses used for the previous temporal estimation experiment on the response time and key-press duration series. However, the analyses are now presented in a different order for expository reasons. The spectral analyses eliminated response times less than 10ms, greater than 2 seconds, and beyond 3 *SD* from the series mean.

#### **3.2.1 Spectral analyses**

From the perspective of fractal scaling, the findings from this study are largely consistent with previously reported findings in the literature on  $1/f$  scaling in simple reaction time (e.g., Holden et al., 2011; Van Orden, et al., 2003). Figure 6 depicts the power spectra, aggregated across participants in each condition. As with the temporal estimation study, statistical tests verifying the presence and reliability of fractal scaling and the sine manipulation were omitted from the text for space considerations. The presence of amplitude spike within key-press durations in the frequency range of ISI changes marks the most salient difference in the spectral portraits of simple reaction times and those of the temporal estimation study.

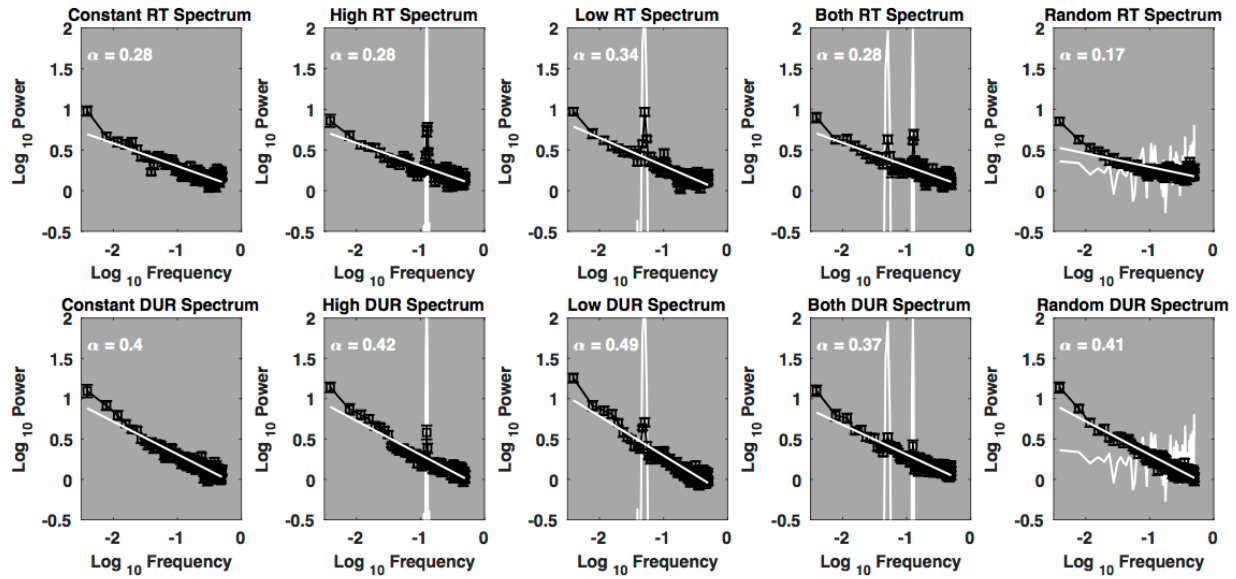


**Figure 6. Aggregate spectral analyses across the five ISI variability conditions.**

Each oscillatory condition reveals a peak in the power spectrum at the frequency of the sine input. The coordination expressed in the simple reaction time task was notably weaker than that in the temporal estimation task, as indicated by the lower amplitude peaks relative to the broadband  $1/f$  scaling. Also, in contrast to temporal estimation performance, the sinusoidal manipulations influenced the key-press duration series. This is indicated by the amplitude spikes embedded in the respective aggregate power spectra at the same frequencies as the sinusoidal inputs.

### 3.2.2 Entrainment alternatives

Next, the entrainment hypothesis is contrasted with the alternative hypothesis that observed coordination resulted from short-range  $-1$  lag correlation rather than entrainment. As with temporal estimation, cross-correlation analyses provide the most direct test of this hypothesis. Figure 7 depicts the results of cross-correlation analyses on both the sinusoidal and random ISI conditions. The  $-1$  lag hypothesis is not generally supported in simple response time. The reaction time and key-press duration series were all uncorrelated with each other at any lag—a single exception being a just-significant  $-1$  lag for the HF cell. Kello et al. (2007) reported a similar absence of lead or lagged associations between response times and key-press durations. An anti-phase short-range error-correction hypothesis posits consistent negative  $-1$  lag associations with the ISIs in all four variable ISI conditions.

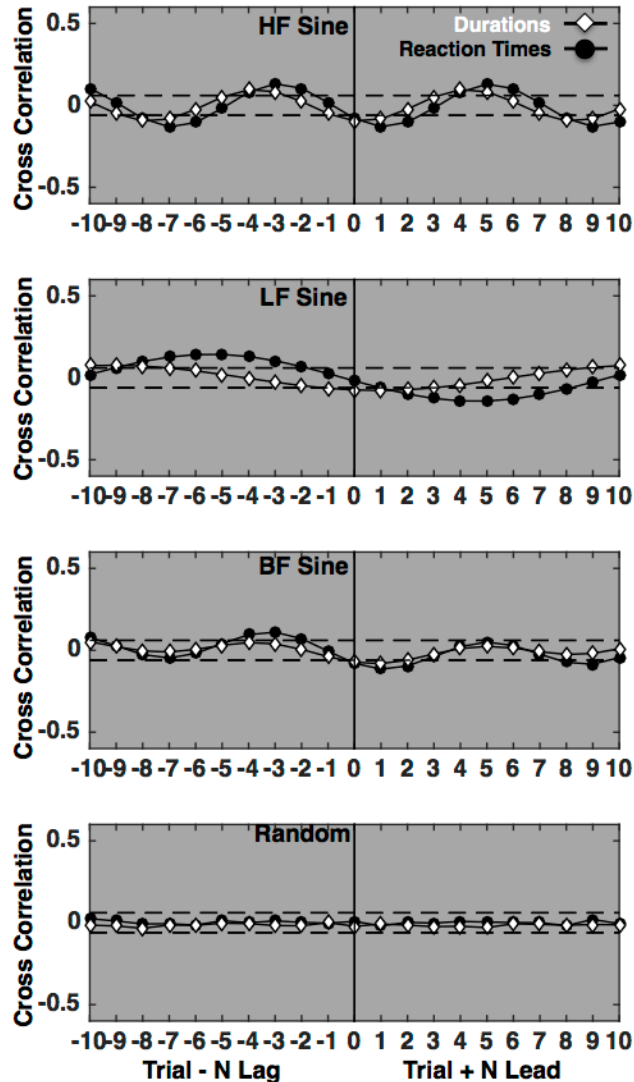


**Figure 7. Response time and key-press duration cross-correlations functions for simple reaction time HF, LF, BF, and random ISI conditions.** *The response times are depicted as filled black circles. The key-press durations are depicted as white diamonds. Reliable positive leads indicate anticipatory associations with the ISI signals, reliable negative lags indicate historical associations the respective ISIs, and a reliable lag-zero indicates a contemporaneous association with an ISI series. The solid vertical line in the center of each plot indicates a zero lag, in which the collected response on the trial was to the presented ISI. The dashed horizontal lines indicate the positive and negative cutoffs for statistical reliability,  $r = \pm .06$  ( $\pm 2 / \sqrt{1090}$ ) that was used for all cross-correlations. The key-press duration cross-correlation functions are depicted as white diamonds in the plots as well. The oscillatory cross-correlations indicate an entrainment pattern across trials in the sinusoid conditions. The response time -1 lag cross-correlations were unreliable in all four of the fluctuating ISI conditions. Detrending all the trial-series prior to the analysis yielded identical cross-correlation outcomes. ISI = Inter-stimulus Interval, HF = High frequency, LF = Low Frequency, BF = Both Frequencies.*

The temporal estimation study indicated that antiphase coordination is the preferred mode of entrainment in these tasks. However, all three sine ISI simple reaction conditions produced reliable antiphase leads with the input sines. The cross-correlation plots indicate a reliable +1 leads for both the response times and durations in

the HF and BF cells. Similarly, it indicates a reliable +4, +5 antiphase lead for the response times and a +1 duration antiphase key-press duration lead. Historically, the tracking and manual control literature recognized similar anticipatory, or open-loop leads, as characteristic of a control strategy that seeks to compensate for intrinsic perceptual-motor delays (see Flach & Jagacinski, 2003). Next, these patterns are examined from the synchronization perspective.

### **3.2.3 Entrainment-based phase shifting**

Figure 8 depicts the averaged HF, LF, and BF response-time and key-press duration performances as a function condition means and phase relations, relative to the input sinusoid. Two short vectors depicting the mean reaction time and mean key-press duration for the HF, LF and BF are drawn as dotted black and white lines, respectively, in plots A, B and C. The angle of each vector represents the measure's relative phase relation to the ISI sine. The solid black vectors represent a composite variable derived from the sum of each participant's response time and key-press durations, and relative phase angles, derived from the cross-correlation analysis (RT+DUR).

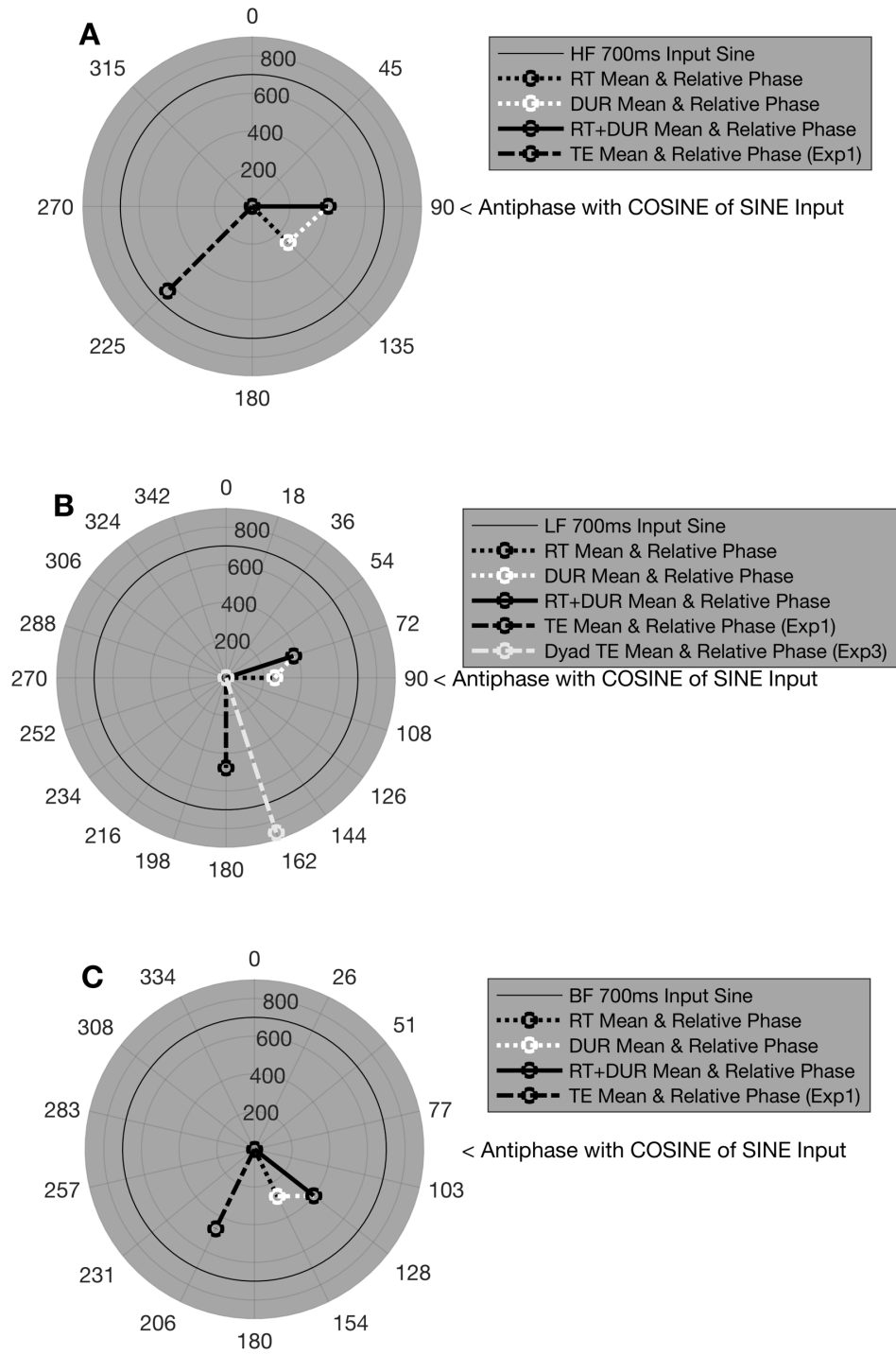


Figure 8. Phase relationship between sinusoidal input and response time, key-

**press duration, and combined response-time key-press trial-series.** *The radius axis of each polar plot represents response time, from the origin to 1000ms at the outer edge of the disk. The plot circumference axis depicts relative phase angles with the sine inputs, in degrees, as a function the relative phases visited on each trial in the period-8, 20, and ~14 ISI sines in plots A, B, and C, respectively. In each polar plot, the 700ms mean of ISI sine input is depicted as a thin, solid black 700ms circle.*

*Plot A depicts the averaged HF response times, keypress durations, and their sum as a function of their location in the 8-trial sinusoid as dashed black, dashed white, and solid black vectors. The summed RT+DUR 90° relative phase relation is antiphase with the input ISI cosine, since the sign of the cross-correlation leads, from which they were derived, are negative. Plot B depicts the averaged LF response times, keypress durations, and their sum as a function of their relative phases in the 20-trial sinusoid as dashed black, dashed white, and solid black vectors. Again, the negative sign of the cross-correlation leads indicates the summed RT+DUR 72° relative phase relation is antiphase with the input ISI cosine. Similarly, plot C depicts the averaged BF response times, keypress durations, and their sum as a function of the relative phases in their mean 14-trial sinusoid as dashed black, dashed white, and solid black vectors. The negative sign of the cross-correlation leads indicates the summed RT+DUR 128° relative phase relation is antiphase with the input ISI cosine.*

*For comparison purposes, the approximately antiphase synchronization of vectors representing the averaged temporal estimation data for the Experiment 1 HF, LF, & BF conditions are depicted as dashed black lines and Experiment 3's LF dyadic condition is depicted as a dashed light gray vector. All told, participants are capable of flexibly assembling their performances to entrain the phase relations indicated by task demands.*

Figure 8 demonstrates how, when combined, the relative phase relations of the individual RT and DUR variables in all three conditions are approximately 90° (¼ cycle,  $M = 96.67^\circ$ ) ahead of the input sine. This particular phase relation is equivalent to a 180° antiphase relation with the cosine of the input sinusoid. The cosine is the input ISI's derivative, indicating its direction and rate of change. Both response times and key-press durations tended to increase as the ISI's got progressively shorter; as the ISI's increased, participants' response times and key-press durations decreased.

Apparently, participants discovered a functional solution to the demands of the task by exploiting within-trial degrees of freedom by entraining their key-press durations. For comparison purposes, vectors depicting mean temporal estimation performance from Experiments 1 & 3 are depicted as dashed black and light gray lines, respectively, in plots A, B, and C. Altogether, the relative phase plots illustrate that participants are capable of maintaining a range of relative phase relations with the input sines. Moreover, the preferred relative phases appear strongly constrained by the details of task demands.

From the perspective of lead/lagged cross-correlations, the documented phase relationships are difficult to square with theories positing exclusively historical short-range error correction as the foundation performance. That is, participants combined the delays entailed in their response times and key-press durations to support antiphase synchronization with the *derivative* of the input sine. The ISI cosines, themselves, were never presented to participants. However, if one allows that unrepresented relational information may support coordinative activity, then the basis of the phase-shifted synchronization is revealed as relatively simple. As the ISIs grew progressively longer, the combined response and duration times tended to accelerate. As the ISIs became progressively shorter, the combined response and duration times tended to decelerate. In fact, the attractor strength analyses reveal that the sinusoidal entrainment of the summed response and duration times (RT+DUR) was more robust than either measure

in isolation, as we report in the next section.

### 3.2.4 Attractor strength and stochastic noise amplitude

The wavelet reconstruction technique described in Experiment 1 was again used to reconstruct signals appropriate for a cross-recurrence analysis. One-way between-subjects ANOVAs, at the level of the separate RT and key-press duration measures, were employed to contrast the lambda ( $\lambda$ ) and noise amplitude ( $Q$ ) levels across each of the three sine conditions with controls. Only the LF (period 20) condition revealed reliably different average lambdas, relative to the constant and random control groups  $F(1, 42) = 11.34$ ,  $r^2 = .22$ ,  $p < .05$ , ( $M_{LF} = .07$ ,  $SD = .02$ ,  $M_{Control} = .05$ ,  $SD = .02$ ). Likewise, only the LF condition revealed a reliable difference in average noise levels ( $Q$ ) in contrast with controls,  $F(1, 42) = 4.24$ ,  $r^2 = .09$ ,  $p < .05$ , ( $M_{LF} = 28$ ,  $SD = 8.85$ ,  $M_{Control} = 34.81$ ,  $SD = 11.08$ ). As predicted, the cross-recurrence analyses indicated weaker overall patterns of sinusoidal entrainment than for temporal estimation.

Identical analyses conducted on the key-press duration series revealed evidence of entrainment. The lambda contrasts were reliable for the HF and LF conditions, as compared to the constant and random controls,  $F(1, 42) = 6.54$ ,  $r^2 = .13$ ,  $p < .05$ , ( $M_{HF} = .035$ ,  $SD = .012$ ,  $M_{Control} = .027$ ,  $SD = .007$ ) and  $F(1, 42) = 6.32$ ,  $r^2 = .12$ ,  $p < .05$ , ( $M_{LF} = .071$ ,  $SD = .029$ ,  $M_{Control} = .054$ ,  $SD = .018$ ) respectively. However, only the  $Q$  noise level for BF condition was reliably reduced, relative to controls  $F(1, 42) = 8.36$ ,  $r^2 = .14$ ,  $p < .05$ , ( $M_{BF} = 102.24$ ,  $SD = 12.80$ ,  $M_{Control} = 118.31$ ,  $SD = 21.15$ ).

That being said, the previous relative phase analysis implicated a *sum* of response time and key-press durations as the fundamental coordinative variable in simple reaction time. We used the summed (RT+DUR) series and repeated the LF one-way between-subjects ANOVAs contrasts of lambda ( $\lambda$ ) and noise amplitude ( $Q$ ) levels with controls,  $F(1, 42) = 36.01$ ,  $r^2 = .43$ ,  $p < .05$ , ( $M_{LF} = .08$ ,  $SD = .02$ ,  $M_{Control} = .05$ ,  $SD = .02$ ) and  $F(1, 42) = 17.29$ ,  $r^2 = .28$ ,  $p < .05$ , ( $M_{LF} = 25.98$ ,  $SD = 5.74$ ,  $M_{Control} = 39.83$ ,  $SD = 12.53$ ) for  $\lambda$  and  $Q$ , respectively. In each analysis the summed variable captured at least twice as much variance as individual variables. Notably, an analysis on the sums also allowed the previously unreliable HF lambda ( $\lambda$ ) contrast to demonstrate significant differences from the control group,  $F(1, 42) = 4.39$ ,  $r^2 = .09$ ,  $p < .05$ , ( $M_{HF} = .032$ ,  $SD = .008$ ,  $M_{Control} = .027$ ,  $SD = .008$ ). Overall, the summed variable maintained stronger, more coherent coordination with the input sinusoid than the response times or duration series alone.

Furthermore, a contrast of the summed LF  $SD\Phi$  frequency detuning variable with controls was reliable,  $F(1, 42) = 24.34$ ,  $r^2 = .35$ ,  $p < .05$ , ( $M_{LF} = 12.95$ ,  $SD = 3.26$ ,  $M_{Control} = 20.79$ ,  $SD = 5.91$ ). Identical analyses using either the response times or the duration series in isolation were not significantly different from controls. In addition, the relationship between participant's mean response time and the  $SD\Phi$  detuning variable was consistent with the more general quadratic relationship between participant's average temporal estimates and  $SD\Phi$ , discussed in Experiment 1. The mean summed RT+DUR and  $SD\Phi$  data pairs are depicted in Figure 4 as black triangles. Their relatively limited average time span is expected in the context of a simple reaction task. Nevertheless, they are consistent with the relationship established by the temporal estimation task. Participants with mean response times (i.e., intrinsic frequencies) closer to the frequency of the sinusoidal oscillation displayed enhanced entrainment. This outcome again implicates both oscillatory dynamics and the RT+DUR collective variable

as fundamental resources for the support of the observed coordinative activity.

### 3.3 Discussion

Overall, relative phases analyses indicated the summed response time and keypress duration signals maintained an approximately antiphase  $\frac{1}{4}$  cycle or  $90^\circ$  relative phase relation with the input sine; one that is equivalent to an antiphase ( $180^\circ$ ) relationship with the cosine of the input ISIs. Presumably, the key-press durations became enfolded into the coordinative dynamic because they offered a route to maintaining an effective coordinative pattern that was otherwise more difficult to maintain by relying exclusively on the response times themselves.

Participants demonstrated a capacity to leverage the degrees of freedom supplied by task constraints and to simultaneously use nonlocal, holistic patterns of change to satisfy task demands. The relative phase analyses revealed how the bulk of this coordinative activity can be understood in terms of the dynamics of coupled oscillators. The results illustrate how theoretical narratives that rely exclusively on instantaneous snapshots of an organism's immediate past do not account for the broad capacity of participants to perceive and exploit environmental patterns.

In this study, the key-press duration series were drawn into the coordinative activity required to accomplish the task. The quantitative differences observed between the temporal estimation in Experiment 1 and simple reaction protocols in Experiment 2 suggest the tasks differed largely by timing and degree, in much the same way as walking and running differ in terms of a synergistic reorganization that occurs with a walk-to-run gait transition (Turvey, 2007). Ostensibly, the same basic perception-action systems are in play, but their roles are reorganized to meet distinct task demands. The observed patterns of coordination differ largely in terms of their relative timescale, and the organization and degree of coupling among the various acts and task events. This suggests that a simple reaction protocol could be reframed as a temporal estimation task in which participants attempt to respond after zero time has elapsed from the onset of the target display.

The difference between temporal estimation and simple reaction is sometimes portrayed as the distinction between cognition and motor control (e.g., Gilden, et al., 1995) or as one that arises from a link between the cognitive timekeeper and the motor system (Wing & Kristoferson, 1973). However, the observed flexible entrainments suggest considering both tasks in terms of a reorganization of what is fundamentally the same system: a perception-action system that discovers and maintains an appropriate organization to accomplish the experimenter assigned task goals. In this way, temporal estimation and simple reaction time performances are plausibly connected across a continuum established by task demands. Next, we revisit temporal estimation and present a study that offers a more direct test of the short-range, independent process hypothesis in temporal estimation.

### 4. Experiment 3: Sinusoidal synchronization in dyadic temporal estimation

Despite evidence in favor of oscillatory entrainment in temporal estimation, one may nevertheless find the concrete -1 lag cross-correlations too compelling to justify overlaying them with a more abstract synchronization hypothesis. This study tested the short-range, dedicated process hypothesis in the context of a dyadic temporal estimation task. Two participants shared a single response keyboard and took turns providing temporal estimates using separate buttons. The left-side participants were

queued with blue signals to respond, and their trials had a constant ITI. The right-side participants responded to red signals, and their trials had the low-frequency 20-trial sine ITI. Otherwise, the temporal estimation procedures and instructions were identical to those of Experiment 1.

The dyadic procedure was designed to reduce the possibility that intrinsic physiological variables were responsible for supporting longer timescale synchronization. Tempered support via variables intrinsic to individuals was expected since successive responses were traded-off between two separate physiological systems. From the short-term error-correction perspective, these circumstances enhanced participants' dependence on short-range perceptual registers, and optimized the conditions for weak anticipation and the reliance on -1 lag information. That is, the short-range prediction was that only information derived from immediate perceptual circumstances was required to maintain any observed coordinative activity. Therefore, the constant ITI participant would not display sinusoidal entrainment, and a simple -1 lag model would be sufficient to capture sine ITI participant's performance.

On the other hand, informationally coupled oscillatory systems have an intrinsic propensity to entrain to each other. As such, the synchronization perspective predicted that reliable entrainment should emerge, even when the task is distributed across distinct individuals and the oscillatory signal was localized to a single individual. Moreover, since the dyadic system's functional capacity was expressed at a distributed level of organization, more robust entrainment was expected at the holistic system level, rather than at the level of the individual participant's performances. This prediction generalized the observation of flexible assembly indicated by superior within-response RT+DUR entrainment in simple reaction time to temporal estimation responding that was distributed across individuals.

## **4.1 Method**

### **4.1.1 Participants**

Sixty-two introductory psychology students participated voluntarily as one of several paths to fulfilling an outside-of-class research requirement. Thirty-one dyads were assembled as two participants signed-up for the same time-slot using a research participation scheduling website. Partial data on four additional dyads was collected but excluded from analyses because not all trials were completed.

### **4.1.2 Apparatus**

The participant seated on the left received a constant 700ms ITI, and the participant seated on the right received a LF sinusoidal ITI with a mean of 700ms ( $SD = 180ms$ ). The study trials were presented using DirectRT for the first eight dyads, and E-Prime was used subsequently. The software change occurred because an author changed laboratories during data collection. All remaining trial events and timing were identical to those described in Experiment 1.

### **4.1.3 Procedure**

Participants were instructed to respond by pressing a keyboard button once they determined the visual stimulus (i.e., #####) had been displayed on the screen for 700ms. To minimize out-of-sequence responses, left-side participants were instructed to respond to a blue stimulus, and right-side participants responded following the presentation of a red stimulus. Blue and red signals were interleaved on every other trial, such that participants took turns responding on the same keyboard. The left-side

responses were recorded on the computer's "z" key, and right-side responses were recorded using the "/" key. Participants responded with their index finger on their preferred hand. Five buffer practice trials were presented, followed immediately by 2,200 experimental trials, or 1,100 for each participant. Just as in the previous studies, participants were not informed about the sine ITIs. Likewise, they were not prompted to coordinate with one another.

## 4.2 Results

### 4.2.1 Spectral analysis

The same temporal estimation censoring procedures described in Experiment 1 were used. However, since the sessions were longer, linear trends were removed for all analyses, and all censored trials were replaced with zeros after the normalization step to maintain intact trial-sequences at both the dyadic and individual levels. Individual participant trial-series were generated by extracting every other trial from the 2,200 trial dyadic series. Odd trials were assigned to the left participant and even trials to the right. Miscued trials were included in all analyses but were too rare to impact the analyses; ten of the 31 dyads made no errors in responding to their blue or red response cues ( $M_{\text{miscues}} = 4$ ,  $SD = 5$ ,  $Max = 21$ ).

Spectral analyses for the individual series used the 127-frequency spectrum, and a 255-frequency spectrum was used for the 2,200 dyadic series in order to equate the size of the sample averages used to estimate power at each frequency. The specific frequency coefficients generated in the analyses were equated by truncating the initial 76 and 151 observations in the individual and dyadic trial-series, respectively, yielding trial-series of 1,024 and 2,048 observations, respectively.

A one-way repeated measures ANOVA revealed a reliable difference among the average scaling exponents that characterized each performance category,  $F(2,60) = 4.05$ ,  $r^2 = .12$ ,  $p < .05$ . Pairwise post-hoc contrasts, using Tukey's HSD to control for family-wise error rates revealed the sine ITIs scaling exponents (right participant) were weakened (whitened), relative to the dyadic time-series,  $F(1,30) = 12.37$ ,  $r^2 = .29$ ,  $p < .05$ ,  $M_{\text{left}} (SD) \alpha = .60 (.18)$ ,  $M_{\text{right}} (SD) \alpha = .53 (.15)$ ,  $M_{\text{dyad}} (SD) \alpha = .64 (.13)$ . This outcome was not explicitly predicted but is consistent with previous demonstrations that extrinsic sources of variability tend to whiten  $1/f$  scaling (e.g., Holden et al., 2011; Van Orden et al., 2003).

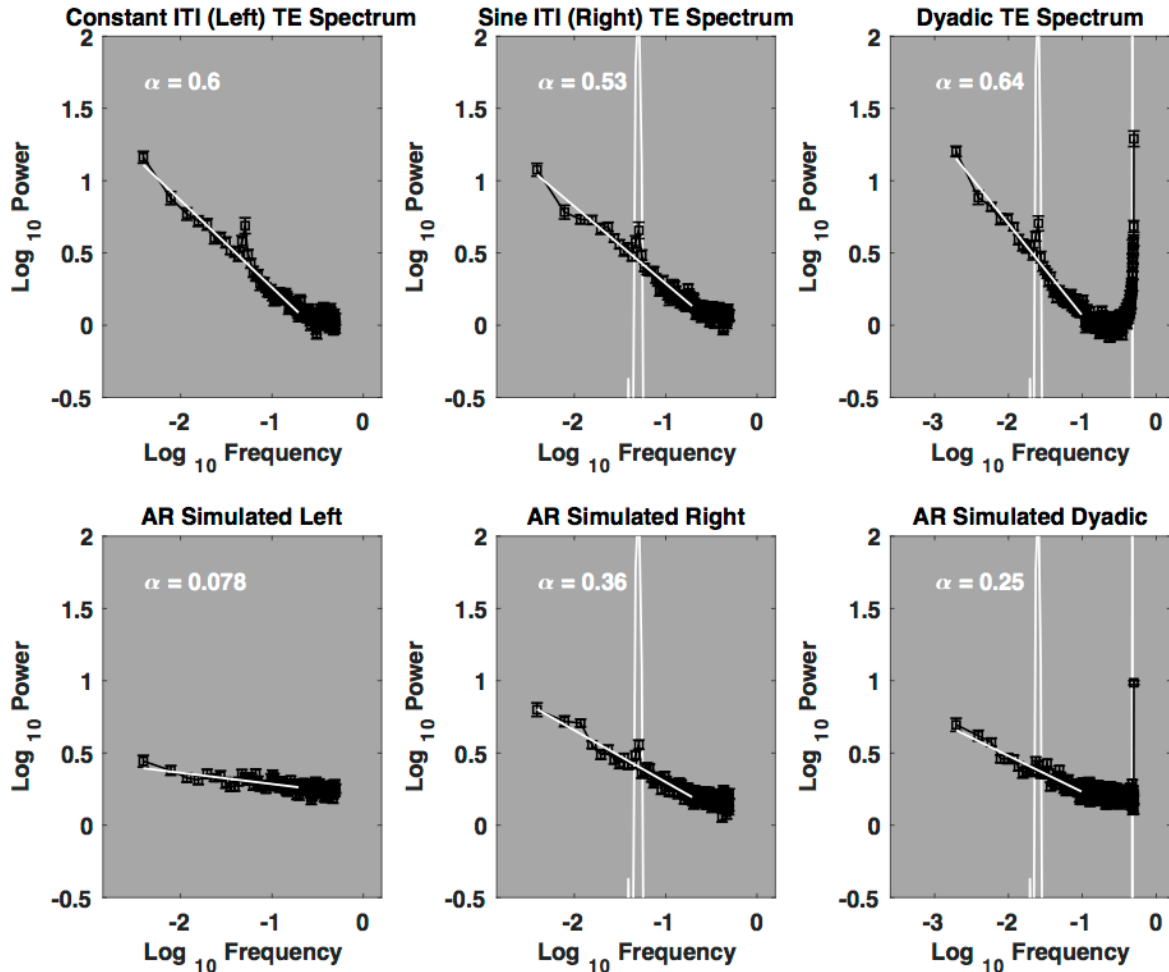


**Figure 9. Empirical and AR-simulated power spectra of dyadic temporal estimation trial-series.** The upper left plot depicts the left-side participants' averaged power spectrum. The upper center plot depicts the right-side participants' averaged power spectrum. Note the spike in the left-side spectrum at the same frequency in which the ITI sine was presented to the participants on the right. The plot on the upper right depicts the dyads' averaged power spectrum. The longer 2,200 series allowed a lower frequency of change of .0019, or every 512 trials to be computed. Notably, the  $1/f$  pattern reliably persists on timescales of change up to approximately 15 minutes. Thus, events that are about 700ms in duration display long-range dependence across a time span of about 900,000ms. The interleaving of the constant sinusoidal ITIs shifted the spectral spike to .025, a 40-trial period. The high-frequency spike in the input ITI signal, depicted in white, resulted from interleaving the constant and sinusoid ITIs. Cross-correlation analyses indicated the short-range spike in the dyadic series arose as a consequence of a negative correlation between participant's successive temporal estimates that is symptomatic of error correction. The three lower plots depict the averaged AR simulation power spectra for comparison. The AR model does not approximate the empirical scaling or spectral spikes very well since it is equivalent to a smoothing operation. Identical simulation outcomes resulted when the fractal scaling was synthesized from the dyadic temporal estimation time-series themselves, using an iterated amplitude adjusted Fourier transform algorithm (Schreiber & Schmitz, 1996). AR= Autoregressive, ITI = Inter-Trial-Interval.

The three error-bar plots in Figure 9 illustrate averaged dyadic temporal estimation scaling relations for the Constant ITI participants (left), Sinusoidal ITI

participants, (center) and the complete dyad (right). First, the left spectral plot displays a clear period-20 spectral peak, indicating the participants seated on the left and receiving constant ITIs entrained to the sinusoid presented only to their counterparts on the right. The center plot expressed a period-20 spectral spike as well, indicating the right-side participants also entrained to the ITI sinusoid. Finally, the dyad's spectrum, based on the final 2,048 trials expressed two spectral spikes, one at period-40, the other on the far right, at period-2, or every other trial.

Since the constant and sinusoidal ITIs were interleaved, the period of the ITI sine was doubled to 40 trials, explaining the period-40 spike. Likewise, the alternation between participant responses across successive trials introduced a strong high frequency spectral spike as well. It is not evident in the individual participant's plots because it is above their highest sampled frequency. The basis of the empirical high-frequency spike, on the right side of the dyad spectrum, was an anti-correlation between participants resulting from short-term error corrections directed at accommodating their partner's temporal estimates across trials. For example, while the dyads themselves displayed a wide range of temporal estimates ( $M = 852$ ,  $SD = 169$ ,  $Range = 843$ ) the temporal estimates of individuals that comprised the dyads were strongly correlated,  $F(1,30) = 31.48$ ,  $r^2 = .52$ ,  $p < .05$ .

By contrast, the dyad's scaling exponents, a broadband measure of correspondence in their temporal variability, were uncorrelated. Given the dyadic study was designed to enhance reliance on short-term information, the absence of an identical high-frequency spike in the Experiment 1 single-individual temporal estimation task corroborates the earlier proposal that participants did not achieve entrainment strictly or largely by means of short-term sensory information.

#### 4.2.2 Attractor strength and noise amplitude

Analyses on the individual participants used the LF period-20 ITI sinusoid, while the dyadic analysis used a period-40 ITI sinusoid to reflect the alternating constant and sinusoidal ITIs. A one-way repeated-measures ANOVA revealed reliable differences in average attractor strength ( $\lambda$ ),  $F(2,60) = 22.77$ ,  $r^2 = .43$ ,  $p < .05$ ,  $M_{\text{left}} = .07$  ( $SD = .04$ )  $M_{\text{right}} = .06$  ( $SD = .02$ ),  $M_{\text{dyad}} = .12$  ( $SD = .05$ ).

As predicted, the distributed signal expressed more robust entrainment than either the left or right participants alone. A planned contrast of the left participant's and the dyad's average  $\lambda$  was significantly different,  $F(1,30) = 22.38$ ,  $r^2 = .43$ ,  $p < .05$ . The same contrast on the right participant's average  $\lambda$  values revealed a reliable difference as well,  $F(1,30) = 48.77$ ,  $r^2 = .62$ ,  $p < .05$ . The relative entrainment strength at the dyadic level was almost double that expressed at the individual levels. This suggests both participants entrained at the dyadic level, while simultaneously accommodating each other, despite the fact that only one participant's ITIs were sinusoidal.

Finally,  $SD\Phi$  frequency detuning values were computed at the individual level of participants and the distributed level of dyads. The black squares plotted on the left plot in Figure 4 illustrate that the dyadic  $SD\Phi$  was consistent with the detuning hypothesis discussed in Experiment 1. Dyads with mean temporal estimates closer to the 700ms average period of the sine ITI expressed stronger entrainment. A quadratic regression, that included both averaged Experiment 1 individual and Experiment 3 dyadic temporal estimates as predictors, and their respective  $SD\Phi$  values as dependent variables, revealed a reliable quadratic relationship,  $F(2,99) = 23.29$ ,  $r^2 = .32$ ,  $p < .05$ . By contrast,

the same analysis, substituting quantities derived at the level of the individual Experiment 3 performances failed to yield a reliable relationship. This dissociation again suggests the observed coordinative activity was maintained at the dyadic level, and does not reduce to the individual synchronization patterns.

#### **4.2.3 Entrainment alternatives**

Except for the use of quadratic detrending to enhance stationarity, the spectral censoring procedures described above were similarly applied to the cross-correlation analyses plotted in Figure 10. They revealed an anti-phase +1 lead as the dyad's maximum correlation with a 40-trial period ITI sine wave, and as the peak correlation of the 20-trial period sine with the left and right individual's trial-series. In addition, the cross-correlation analysis suggested broad multi-trial associations between the left and right participant's trial-series. These cross-correlation patterns all suggest multi-trial coordination and anticipatory relationships rather than discrete -1 lag autocorrelations. Nevertheless, we now consider the possibility that the observed long-term synchronization was supported by strictly short-term error corrections.

The dyadic study was designed to encourage reliance on -1 lag information sources. All 31 dyad trial-series were averaged together and then differenced to check for the -1 lag effects implicated in the dyadic power spectrum. A partial autocorrelation analysis on the differenced series revealed a reliable -1 lag negative autocorrelation of -.68 between the averaged left and right trial-series. Likewise, the -1 lag partial autocorrelations for the averaged left and right trial-series were both positive and reliable, at .51 and .48, respectively. These relationships served as entry points for the design of a short-range -1 lag model that included four -1 lag correlations: The left- and right-side participant's negative relationship and both participant's relationship with their immediately preceding ITI. Since the left participant received constant ITIs, their -1 lag correlation related their present response to their previous response; the right participant's response included a -1 lag self-correlation and a previous sine ITI correlation. The magnitudes of the individual correlations were adjusted to approximate the observed aggregate correlations and approximate the empirical cross-correlations. As in Experiment 1, each dyad's  $1/f$  scaling was built into the model by matching it with a synthetic signal and using it as the basis for each synthetic dyad's AR model run.

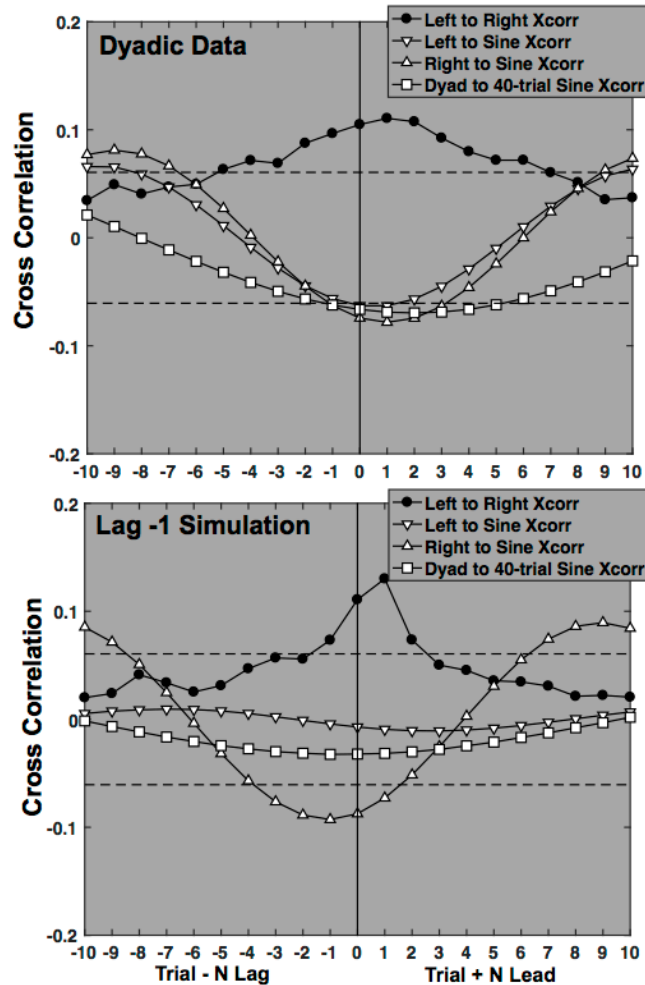


**Figure 10. Fit between -1 lag model and empirical data from dyadic temporal estimation task.** The upper plot portrays the empirical dyadic cross-correlation functions. The black circles depict the cross-correlations of dyad members. Members of a dyad track each other across a range of leads and lags. The upward pointing white triangles depict the left participants' association with the 20-trial sine ITI, the downward-pointing triangles depict the right participants', and the white squares depict the dyadic trial-series entrainment with a 40-trial period sinusoid. The lower plot depicts the cross-correlation analysis for a -1 lag model. It fails to capture the general anticipatory entrainment in the empirical series, as well as "transmit" the sinusoidal entrainment to the left or dyadic trial-series.

Figure 10 depicts both the empirical cross-correlations, and those of a representative -1 lag model. In terms of the right-side participant, the -1 lag model displays an expected -1 lag anti-correlation with the sine ITI and the simulated right-side data, but the pattern conflicts with the +1 lead evident in the empirical data. Also, the -1 lag anti-correlation between the simulated left- and right-side responses manages a maximum lead +1 association that is qualitatively similar but briefer and more peaked than the empirical relationship. These count as minor discrepancies between the short-range model and the empirical patterns. The discrepancies between the observed and -1 lag model for left and dyadic performances are more significant.

Comparable strength anticipatory +1 lead entrainments are evident in the

empirical left and dyadic series, in addition to the right series that was presented with the sine ITI. However, despite the cross-participant -1 lag anti-correlation built into the model, these patterns are absent from the -1 lag simulations. The short-range account is unable to “transmit” sinusoidal coordination from the right to the left side of the simulated dyad. This explains the relative correlation strength rank-ordering in the simulations: The right series tracks the sine ITI, and the left series lacks coordination with the sine ITI. The simulated dyad expresses intermediate strength correlation with the sine ITI, resulting from averaging the simulated right and left sides rather than entrainment. By contrast, the empirical left, right, and dyadic all express similar and reliable +1 leads. Clearly the participants’ performances and the model simulation employ different routes to achieve coordination with the ITI sine.

### 4.3 Discussion

The recurrence analyses implicated the dyadic level 40-trial sinusoidal entrainment as the likely basis for synchronization. Notably, a 40-trial sine pattern was never presented to either individual participant. It is a global pattern that is explicitly disrupted at the level of individual trials since it is interleaved with constant ITIs, resulting in a two-trial high-frequency oscillation that participants largely ignore in favor of coordination with the global oscillation and each other. In contrast, the AR model failed to reproduce the dynamics present in the dyadic and individual trial-series. Moreover, the model’s short-term emphasis imposes a strong tendency to over-whiten the simulated trial-series by acting as a smoothing operator.

Perhaps one could suggest a post-hoc short-range narrative for these results. For instance, the right-side participant might use a -1 lag to track the sine, and the left participant might track the sine using a lag -2 copy of the ITI. However, proposals like this one raise additional issues. First, they undermine the assumption of the priority of short-range information. Second, it is unclear why participants would adopt different approaches to completing the same activity. Third, if one proposes that participants peruse multiple sources of short-term information from which to build their performance, then why choose the sine wave over the constant ITI? The constant ITI is a far better signal from which to generate consistent temporal estimates.

On the other hand, the synchronization perspective suggests that dyad members become informationally-linked oscillatory systems that have an inherent propensity for entrainment. Both participants possess an inherent capacity to simultaneously tune their activity to each other and to the overall sinusoidal pattern, even in the face strong perturbations unfolding on the fastest timescales of change in dyadic temporal estimation. Furthermore, the performances were anticipatory, and the seat of the coordinative activity was distributed between both individuals at the dyadic level. This is a concrete example of emergent and distributed cognition (see Figure 11). Overall, the results are reminiscent of the established capacity for spontaneous intra- and interpersonal coordination in the movement and motor control literature (e.g., Amazeen, Schmidt, & Turvey, 1995; Haken, Kelso, Bunz, 1985; Schmidt & Richardson, 2008).

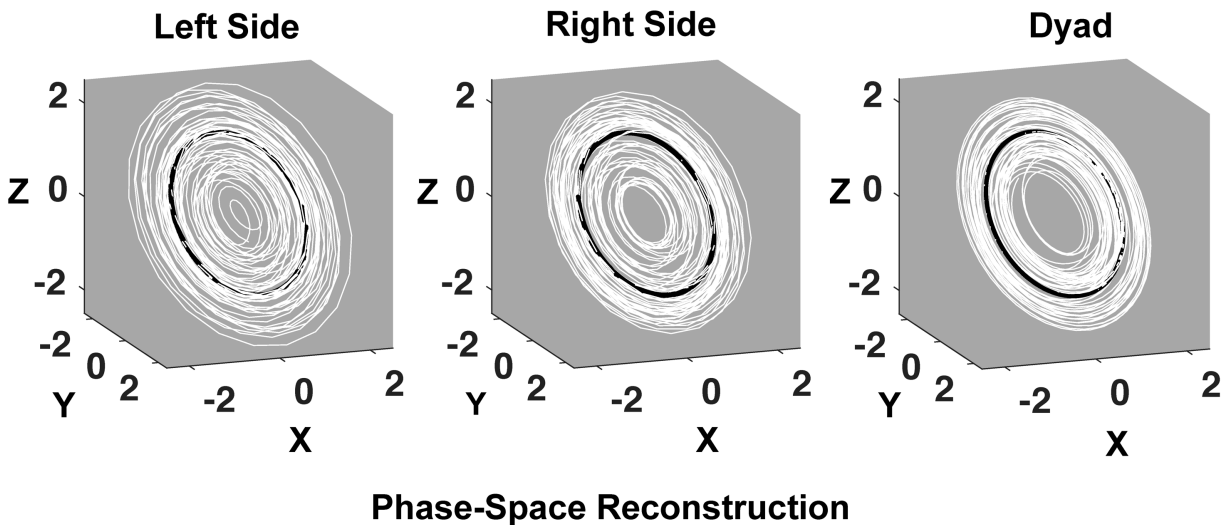


**Figure 11. Left, Right, and Dyadic Phase Spaces.** *The three-dimensional phase space reconstructions of the normalized and averaged left and right time series, as well as the averaged dyadic series are depicted on identical 3-D axes as white lines. The sinusoidal input signals are plotted as black lines in the center of the 3-D axes. The trajectory of the dyadic attractor is smoother and more compact than the individual participant trajectories. This illustrates emergence: the distributed performance is more stable and compact than the component performances from which it is comprised.*

A recently described complexity matching hypothesis may be relevant to the dyadic temporal estimation results, as it can be motivated by some of the synchronization phenomena discussed in the introduction (see Abney, Paxton, Dale, & Kello, 2014; West, Geneston, & Grigolini, 2008). Complexity matching is a statistical physics phenomenon that is pertinent to the coordinative behavior of informationally-coupled complex systems, especially complex networks expressing  $1/f$  scaling in their outputs. The complexity matching hypothesis predicts that both systems will tune to identical  $1/f$  scaling exponents as a consequence of coupling, because identical scaling exponents maximize information exchange between the systems. For example, Abney et al. framed conversations between two individuals as an informational coupling between two complex systems and found support for this pattern in measures of the scaling describing the distribution inter-event-intervals of the speaker's utterance onsets.

Presumably, the complexity matching hypothesis predicts that individual participant's  $1/f$  scaling exponents comprising each dyad would converge as well. After

all, the pairs of participants are informationally coupled. However, there was no association between the participant's  $1/f$  scaling exponents in the present sinusoidal version of the task. Evidence for the same association was similarly absent in a condition in which both dyad members received constant 700ms ITIs (Amon, 2016). However, Amon also implemented a random ITI dyadic temporal estimation condition, in which the left-side participant's ITI was constant and the right-side participant's ITIs varied randomly across trials. The method was otherwise identical to the dyadic study presented in this article. In that condition, the dyad member's  $1/f$  scaling exponents became strongly correlated,  $r^2 = .76$ ,  $p < .001$ . Together, the outcomes of both Abney et al. (2014) and Amon suggest the expression of complexity matching depends on the details of the experimental task used in laboratory studies of human performance. Aspects of method and design control the capacity and categories of informational coupling that are available to be exploited by participants (see also Almurad, Roume, & Delignières, 2017; Delignières, Almurad, Roume, & Marmelat, 2016; Holden et al., 2011).

## 5. General Discussion

Taken together, these three studies established a multi-scale propensity for coordinative activity in cognitive performances. The simple response-time task illustrated the pattern at timescales faster than individual trials. The individual temporal estimation task illustrated the same capacity on timescales much slower than individual trials. Finally, the dyadic task illustrated a capacity for coordinative activity that is distributed across distinct individuals.

Traditionally, the between-trial event sequences of standard self-paced temporal estimation tasks were thought to supply mostly unsystematic error variance to within-trial interval estimation (e.g., Vorberg & Scholze, 2002). Likewise, simple reaction trials were thought to be governed by basic perceptual thresholds in conjunction with largely ballistic response processes that unfold within trials (e.g., Luce, 1986). However, in the present temporal estimation and simple reaction time tasks, participants appeared to leverage the regularity of the oscillatory ITI and ISI manipulations *across* trials to constrain their *within-trial* temporal estimation and simple reaction time performances.

While locally lagged correlations are often symptomatic of coordination, they needn't serve as the sole basis for that activity (see Figure 5). For instance, the association between participants' preferred temporal intervals and the strength of the resulting sinusoidal ITI resonances suggests that temporal estimation performance is influenced by extrinsic oscillatory patterns. The complex phase-shifted relationships that emerged among the simple reaction times and key-press durations supported a global  $90^\circ$  phase relation with the low-frequency driving ISI sinusoid. The surrogate-reconstructed phase-spaces indicated the presence of coordinative trajectories that shared coherent state-space relations and derivatives with the input sinusoids. Entrainment in dyadic temporal estimation was distributed across two individuals. Ultimately, we do not wish to argue that participants cannot support coordination by leveraging short-range information; instead we established that short-range correlation does not exhaust human capacities for coordinative activity (see also Flach, 1990; Jagacinski & Flach, 2003).

Notably, all the coordinative trajectories were embedded in a background of  $1/f$  scaling. The amplitude of the lowest frequency  $1/f$  fluctuations was always larger or at

least as large as the oscillatory amplitudes. In the -1 lag temporal estimation model, the nonstationarity of an additive source of  $1/f$  scaling amplified the magnitude of the sinusoidal coupling while simultaneously nullifying the -1 lag autocorrelation with the randomized ITI series. A similar -1 lag model of the dyadic performances over-whitened the resulting trial-series. The empirically observed performance data did not express these patterns. In other words, -1 lag temporal estimation models were unable to replicate or even preserve the robust scaling relationships commonly observed in temporal estimation tasks. These results suggest that cognitive activity should not be construed as something that is simply added on top of, and independent of  $1/f$  scaling (see Holden et al., 2011; cf. Wagenmakers, 2004; 2005). Instead, scaling is symptomatic of the coordinative dynamics of mind and body necessary to achieve the task at hand.

EEG and fMRI studies commonly reveal the coexistence of  $1/f$  scaling and regular oscillatory fluctuations in low-level brain and nervous system dynamics. For instance, the approximately 11 Hz alpha waves, once thought to indicate a relaxed state of mind, are embedded within broadband  $1/f$  scaling, much as the ITI and ISI entrainments were embedded in  $1/f$  scaling. It is plausible that the core basis of our experimental outcomes resulted from the generic coordinative capacities of an electrochemically coupled complex system, such as the human brain, body, and nervous system. In the case of temporal estimation or simple reaction time, this basic coordinative capacity leverages regular patterns in the environment in order to support and maintain performance across successive trials.  $1/f$  scaling is relatively robust in human cognition and performance, such that broadband whitening of what would otherwise be  $1/f$  scaling in cognitive tasks is expressed only by introducing sources of functional uncertainty to task and method (e.g., random versus constant ITIs and ISIs, more versus fewer response options, more difficult versus easier judgments, and less skilled versus more skilled participants; Amon & Holden, 2016; Castillo, Kloos, Holden & Richardson, 2015; Experiments 1 & 2; Holden et al., 2011; Kello et al., 2007; Wijnants et al., 2009; Ward, 2002).

### **5.1 Temporal estimation models**

The contemporary prospective control literature distinguishes between strong and weak anticipation. Weak anticipation theories rely on encapsulated, analytic processes, such as the discretely lagged autocorrelation model described by Torre and colleagues (2013). Historically, timing and time perception researchers implemented weak anticipation with mechanisms that spanned a continuum from centralized internal-clocks (e.g., Wing & Kristofferson, 1973) and accumulator/counter models (e.g., Grondin, 2005) to large networks of stable oscillators (e.g. Church & Broadbent, 1990; for review see Grondin, 2010). These dedicated systems served as internal temporal references that supported cognitive and perceptual error corrections during ongoing timing performance. A range of cognitive resources, such as attention, memory, and even specific perceptual modalities were considered as origins for potential timing mechanisms (e.g., Brown & Boltz, 2002; Ornstein, 1969; Johnston, Arnold, & Nishida, 2006). Regardless of the details of their psychological motivation, formal timing models that entail discrete comparator stages to support error corrections are consistent with weak anticipation as their time-series can be approximated -1 lag AR and related short-range models representing local cognitive or environmental states that are limited to

immediate behavioral consequences.

Strong anticipation theories emphasize holistic control solutions that entail interdependent agent-environment coordination in which timing behavior emerges as a consequence of intrinsic behavioral dynamics and the details of environmental circumstances. That is, effective control is not reduced to the activities of discrete or dedicated sub-systems. Instead, control is thought to be an emergent consequence of an inclusive global organization that is supported by interdependent and flexible dynamic coupling among many bodily and nervous system processes (e.g., Balasubramaniam, 2006; Experiment 2 & 3; Marmelat, & Delignières, 2012; Stephen et al., 2008; Stepp & Turvey, 2010; Zelaznik, Spencer, & Ivry, 2008).

The results of the present studies favor a global narrative as a basis for the observed performances. Neither the temporal estimation nor the simple reaction tasks imposed any necessity that our participant's performances accommodate the fluctuating ITI or ISI series. As such, the ITI and ISI signals are strictly irrelevant to model solutions that are governed by encapsulated control strategies. By contrast, the nature of the relatively holistic observed agent-environment coordination suggests an inherent capacity for reliable environmental constraints to become entangled with performance (Holden et al., 2011). That is, cognitive activity is "sticky"—it spontaneously entrains to functional and environmental regularities across a range of timescales. This suggests the nature of the coupling expressed in many cognitive activities is context dependent and emergent in that its expression complies with subtly changing task demands (Van Orden, Kello, & Holden 2010).

## 5.2 Conclusions

The findings demonstrate that punctate, discretely measured response times reflect the impact of coordination and entrainment principles. The oscillatory dynamics of the nervous system are similarly mediated by a host of largely punctate electrochemical events. The nervous system is an excitable medium that is enacted from vast networks of electrochemically-coupled neurons. Neuron populations exploit this capacity to synchronize their activities through energetic flow fields, rather than strictly kinetic Newtonian forces. Nonetheless, the mathematical techniques, originally developed to describe force-based synchronization among physical pendula, are widely used to understand synchronization in systems that are mediated by electrical, chemical, and informational couplings (Richardson, Garcia, Frank, Gregor, & Marsh, 2012; Strogatz, 2003; Winfree, 2001). Thus, entrainment principles hold promise as guides for cognitive modeling activities. Absent guiding scientific principles, cognitive modeling risks becoming a purely descriptive enterprise (cf., Torre & Wagenmakers, 2009).

Recently, cognitive neuroscientists identified pervasive complex functional and neurophysiological networks with the help of fMRI techniques (e.g., Sporns, 2011; 2012). Rhythmic dynamics are implicated in their organization and re-organization in-line with changing task demands (Fries, 2015; Thute et al., 2012). While more research is needed to investigate the properties of these networks, it is possible that complex neurophysiological network dynamics underpin a variety of aspects of human thought and action. In short, oscillatory dynamics may be the glue that binds mind, body, and environment into persistent, coherent, and flexible behavioral trajectories (Kelso, 1995; Bressler, & Kelso, 2001). If that is the case, then it is plausible to maintain a working

hypothesis that the dynamics observed in measurements of response time originate in, or at least echo, the dynamics of supporting biological and neurophysiological processes. In this way, response-time measurements can be reasonably viewed as punctate measurements of underlying and ongoing neurophysiological dynamics.

Our participant's performances captured, accommodated, and likely exploited the inserted sinusoidal test signals. This outcome adds credibility to the hypothesis that  $1/f$  scaling is a product of coordination among the neurophysiological, bodily, and environmental circumstances that support performance. The fact that this ongoing coordinative activity captured the sinusoidal manipulations indicates that processes spanning many timescales of activity serve as resources in supporting goal-directed action. One implication is that intrinsic fractal fluctuations facilitate entrainment to environmental regularities (Hasselmann, 2015). Biological processes are quasi-regular at best, and their mutual entrainments are imperfect (Buzsáki, 2006). Nevertheless, the observed entrainment with the sinusoidal signals corroborates dynamical narratives that view coordinative activity as a foundational source of support for human cognition and action (e.g., Abney, et al., 2014; Holden & Rajaraman, 2012; Järvillehto, 1998; Kelso, 1995; Kello, et al., 2007; Rigoli et al., 2014; Riley & Holden, 2012; Spivey, 2006; Stephen et al., 2008; Stepp & Turvey, 2010; Turvey, 2007; Tschacher & Dauwalder, 2003; Van Orden et al., 2003; Wijnants, 2014; Wijnants et al., 2009; 2012).

## **6. Acknowledgements**

We thank Gerardo Ramirez for help with Experiment 1 & 2 data collection. A portion of the data in Experiment 3 appeared in Mary Jean Amon's PhD dissertation.

## 7. References

- Abarbanel, H. (2012). *Analysis of observed chaotic data*. New York, NY: Springer Science & Business Media.
- Abney, D. H., Paxton, A., Dale, R., & Kello, C. T. (2014). Complexity matching in dyadic conversation. *Journal of Experimental Psychology: General*, *143*, 2304-2046.
- Almurad, Z. M. H., Roume, C., & Delignières, D. (2017). Complexity matching in side-by-side walking. *Human Movement Science*, *54*, 125-136.
- Amazeen, P. G., Schmidt, R. C., & Turvey, M. T. (1995). Frequency detuning of the phase entrainment dynamics of visually coupled rhythmic movements. *Biological Cybernetics*, *72*(6), 511-518.
- Amon, M. J. (2016). *Examining coordination and emergence during individual and distributed cognitive tasks*. (Unpublished doctoral dissertation). University of Cincinnati.
- Amon, M. J. & Holden, J. G. (2016). Fractal scaling and implicit bias: A conceptual replication of Correll (2008). *Proceedings of the 38th Annual Conference of the Cognitive Science Society*. In A. Papafragou, D., Grodner, D. Mirman, & J. C Trueswell (Eds.), *Proceedings of the 38th Annual Conference of the Cognitive Science Society* (pp. 1553-1558). Austin TX: Cognitive Science Society.
- Balasubramaniam, R. (2006). Trajectory formation in timed rhythmic movements. In M.L. Latash & F. Lestienne (Eds), *Progress in Motor Control* (pp. 47–54). New York, NY: Springer.
- Bühner, M., Sparrer, B., & Weitkunat, R. (1987). Interval timing routines for the IBM PC/XT/AT microcomputer family. *Behavior Research Methods, Instruments, & Computers*, *19*, 327-334.
- Bressler, S. L., & Kelso, J. S. (2001). Cortical coordination dynamics and cognition. *Trends in cognitive sciences*, *5*, 1, 26-36.
- Buzsáki, G. (2006). *Rhythms of the brain*. Oxford, England: Oxford University Press.
- Buzsáki, G., & Draguhn, A. (Jun 25, 2004). Neuronal oscillations in cortical networks. *Science*, *304*, (5679), 1926-1929.
- Castillo, R. D., Kloos, H., Holden, J. G., & Richardson, M. J. (2015). Fractal coordination in adults' attention to hierarchical visual patterns. *Nonlin. Dyn. Psychol*, *19*, 147-172.
- Church, R. M., & Broadbent, H. A. (1990). Alternative representations of time, number, and rate. *Cognition*, *37*(1), 55-81.
- Delignières, D., Almurad, Z.M.H., Roume, C. & Marmelat, V. (2016). Multifractal signatures of complexity matching. *Experimental Brain Research*, *234*, (10), 2773-2785. DOI: 10.1007/s00221-016-4679-4.
- Flach, J. M. (1990). Control with an eye for perception: Precursors to an active psychophysics. *Ecological Psychology*, *2*, 83-111.
- Fries, P. (2015). Rhythms for cognition: communication through coherence. *Neuron*, *88*, (1), 220-235.
- Gibbs Jr, R. W. (2005). *Embodiment and cognitive science*. Boston, MA: Cambridge University Press.

- Gilden, D. L. (2001). Cognitive emissions of  $1/f$  scaling. *Psychological Review*, 108, 33-56.
- Gilden, D. L. (2009). Global model analysis of cognitive variability. *Cognitive Science*, 33, 1441-1467.
- Gilden, D. L., Thornton, T., & Mallon, M. W. (1995).  $1/f$  scaling in human cognition. *Science*, 267, 1837-1839.
- Glass, L. (2001). Synchronization and rhythmic processes in physiology. *Nature*, 410(6825), 277-284.
- Grondin, S. (2005). Overloading temporal memory. *Journal of Experimental Psychology: Human Perception and Performance*, 31(5), 869.
- Grondin, S. (2010). Timing and time perception: a review of recent behavioral and neuroscience findings and theoretical directions. *Attention, Perception, & Psychophysics*, 72, 3, 561-582.
- Haken, H., Kelso, J. S., & Bunz, H. (1985). A theoretical model of phase transitions in human hand movements. *Biological Cybernetics*, 51, 347-356.
- Hasselmann, F. (2015). Classifying acoustic signals into phoneme categories: average and dyslexic readers make use of complex dynamical patterns and multifractal scaling properties of the speech signal. *PeerJ*, 3, e387.  
<https://doi.org/10.7717/peerj.837>
- Helfrich, R. F., & Knight, R. T. (2016). Oscillatory dynamics of prefrontal cognitive control. *Trends in cognitive sciences*, 20, (12), 916-930.
- Holden, J. G. (2005). Gauging the fractal dimension of cognitive performance. In M.A. Riley & G.C. Van Orden (Eds). *Tutorials in Contemporary Nonlinear Methods for the Behavioral Sciences Web Book* (pp. 267-318). Retrieved May 1, 2015, from <http://www.nsf.gov/sbe/bcs/pac/nmbs/nmbs.jsp>
- Holden, J. G., Choi, I., Amazeen, P. G., & Van Orden, G. (2011). Fractal  $1/f$  dynamics suggest entanglement of measurement and human performance. *Journal of Experimental Psychology: Human Perception and Performance*, 37, 935-948.
- Holden, J. G., & Rajaraman, S. (2012). The self-organization of a spoken word. *Frontiers in Psychology*, 3:209. doi: 10.3398/fpsyg.2012.00209.
- Holden, J. G., Van Orden, G. C., & Turvey, M. T. (2009). Dispersion of response times reveals cognitive dynamics. *Psychological review*, 116, 318-342.
- Huygens, C. (1673/1986). *Horologium oscillatorium. The pendulum clock or geometrical demonstrations concerning the motion of pendula as applied to clocks* (trans, R.J. Blackwell), Ames, IA: Iowa State University Press.
- Izhikevich, E.M. (2007). *Dynamical systems in Neuroscience: The geometry of excitability and bursting*. Cambridge, MA: MIT Press.
- Jagacinski, R. J., & Flach, J. M. (2003). *Control theory for humans: Quantitative approaches to modeling performance*. Boca Raton, FL: CRC Press.
- Järvillehto, T. (1998). The theory of the organism-environment system: I. Description of the theory. *Integrative Physiological and Behavioral Science*, 33: 321-334.
- Jensen, H. J. (1998). *Self-organized criticality: emergent complex behavior in physical and biological systems* (Vol. 10). Cambridge university press.
- Johnston, A., Arnold, D. H., & Nishida, S. (2006). Spatially localized distortions of event time. *Current Biology*, 16, 472-479.
- Kello, C. T., Beltz, B. C., Holden, J. G., & Van Orden, G. C. (2007). The emergent

- coordination of cognitive function. *Journal of Experimental Psychology: General*, 136, 551.
- Kelso, J. A. S. (1995). *Dynamic patterns: The self-organization of brain and behavior*. Cambridge, MA: MIT Press.
- Kiefer, A. W., Riley, M. A., Shockley, K., Villard, S., & Van Orden, G. C. (2009). Walking changes the dynamics of cognitive estimates of time intervals. *Journal of Experimental Psychology: Human Perception and Performance*, 35, 1532-1541.
- Kugler, P. N., & Turvey, M. T. (1987). *Information, natural law and the self-assembly of rhythmic movement*. Hillsdale, NJ: Lawrence Erlbaum and Associates.
- Luce, R. D. (1986). *Response times: Their role in inferring elementary mental organization*. New York, NY: Oxford University Press.
- Marmelat, V., & Delignières, D. (2012). Strong anticipation: complexity matching in interpersonal coordination. *Experimental brain research*, 222, 137-148.
- Newton, I. (1686/1729). *Mathematical principles of natural philosophy and his system of the world*, (trans.), 1934, 1962, London, England: PRINCIPIA, Berkeley, CA: University of California Press.
- Pellecchia, G. L., Shockley, K., & Turvey, M. T. (2005). Concurrent cognitive task modulates coordination dynamics. *Cognitive Science*, 29, 531-557.
- Percival, D. B., & Walden, A. T. (2006). *Wavelet methods for time series analysis* (Vol. 4). Cambridge, UK: Cambridge University Press.
- Press, W.H., Teukolsky, S.A., Vetterline, W.T., & Flannery, B.P. (1992). *Numerical recipes in C: The art of scientific computing*. Cambridge, UK: Cambridge University Press.
- Richardson, M. J., Garcia, R. L., Frank, T. D., Gergor, M., & Marsh, K. L. (2012). Measuring group synchrony: A cluster-phase method for analyzing multivariate movement time-series. *Frontiers in Fractal Physiology*, 3, 405. doi: 10.3389/fphys.2012.00405
- Richardson, M. J., Schmidt, R. C., & Kay, B. A. (2007). Distinguishing the noise and attractor strength of coordinated limb movements using recurrence analysis. *Biological Cybernetics*, 96, 59-78.
- Rigoli, L. M., Holman, D., Spivey, M. J., & Kello, C. T. (2014). Spectral convergence in tapping and physiological fluctuations: coupling and independence of 1/f noise in the central and autonomic nervous systems. *Frontiers in human neuroscience*, 8, 713.
- Riley, M. A., & Holden, J. G. (2012). Dynamics of cognition. *Wiley Interdisciplinary Reviews: Cognitive Science*. doi: 10.1002/wcs.1200.
- Schöner, G. (2002). Timing, clocks, and dynamical systems. *Brain and Cognition*, 48, 31-51.
- Schöner, G., Haken, H., & Kelso, J. A. S. (1986). A stochastic theory of phase transitions in human hand movement. *Biological cybernetics*, 53, 247-257.
- Schmidt, R. C., & Richardson, M. J. (2008). Dynamics of interpersonal coordination. In *Coordination: Neural, behavioral and social dynamics* (pp. 281-308). Springer Berlin Heidelberg.
- Schreiber, T., & Schmitz, A. (1996). Improved surrogate data for nonlinearity tests. *Physical Review Letters*, 77(4), 635.

- Spivey, J. (2007). *The continuity of mind*. Oxford, England: Oxford University Press.
- Sporns, O. (2011). *Networks of the brain*. Cambridge, MA: MIT press.
- Sporns, O. (2012). *Discovering the human connectome*. Cambridge, MA: MIT press.
- Sreekumar, V., Dennis, S., & Doxas, I. (2017). The episodic nature of experience: a dynamical systems analysis. *Cognitive science*, *41*, 5, 1377-1393.
- Sreekumar, V., Dennis, S., Doxas, I., Zhuang, Y., & Belkin, M. (2014). The geometry and dynamics of lifelogs: Discovering the organizational principles of human experience. *PloS one*, *9*(5), e97166.
- Stephen, D. G., Arzamarski, R., & Michaels, C. F. (2010). The role of fractality in perceptual learning: exploration in dynamic touch. *Journal of Experimental Psychology: Human Perception and Performance*, *36*, 1161-1173.
- Stephen, D. G., Stepp, N., Dixon, J. A., & Turvey, M. T. (2008). Strong anticipation: Sensitivity to long-range correlations in synchronization behavior. *Physica A: Statistical Mechanics and its Applications*, *387*, 5271-5278.
- Stepp, N., & Turvey, M. T. (2010). On strong anticipation. *Cognitive Systems Research*, *11*, 148-164.
- Strogatz, S. (2003). *Sync: The emerging science of spontaneous order*. New York, NY: Hyperion.
- Thelen, E., & Smith, L. B. (1994). *A dynamic systems approach to the development of cognition and action*. Cambridge, MA: MIT press.
- Thut, G., Miniussi, C., & Gross, J. (2012). The functional importance of rhythmic activity in the brain. *Current Biology*, *22*, (16), R658-R663.
- Tognoli, E., & Kelso, J. S. (2014a). Enlarging the scope: grasping brain complexity. *Frontiers in Systems Neuroscience*, *8*:122. doi: 10.3389/fnsys.2014.00122
- Tognoli, E., & Kelso, J. S. (2014b). The metastable brain. *Neuron*, *81*, 35-48.
- Torre, K., Varlet, M., & Marmelat, V. (2013). Predicting the biological variability of environmental rhythms: Weak or strong anticipation for sensorimotor synchronization? *Brain and Cognition*, *83*, 342-350.
- Torre, K., & Wagenmakers, E. J. (2009). Theories and models for  $1/f^{\beta}$  noise in human movement science. *Human movement science*, *28*, 297-318.
- Torrence, C., & Compo, G. P. (1998). A practical guide to wavelet analysis. *Bulletin of the American Meteorological society*, *79*, 61-78.
- Turvey, M. T. (2007). Action and perception at the level of synergies. *Human Movement Science*, *26*, 657-697.
- Tschacher, W., & Dauwalder, J. P. (2003). *The dynamical systems approach to cognition: concepts and empirical paradigms based on self-organization, embodiment, and coordination dynamics*. River Edge, NJ: World Scientific.
- Van Orden, G. C., Holden, J. G., & Turvey, M. T. (2003). Self-organization of cognitive performance. *Journal of Experimental Psychology: General*, *132*, 331-350.
- Van Orden, G. C., Holden, J. G., & Turvey, M. T. (2005). Human cognition and  $1/f$  scaling. *Journal of Experimental Psychology: General*, *134*, 117-123.
- Van Orden, G. C., Hollis, G., & Wallot, S. (2012). The blue-collar brain. *Frontiers in Physiology*, *3*:207. doi: 10.3389/fphys.2012.00207
- Van Orden, G. C., Kello, C. T., & Holden, J. G. (2010). Situated behavior and the place of measurement in psychological theory. *Ecological Psychology*, *22*, 24-43.
- Van Orden, G. C., Kloos, H., & Wallot, S. (2011). Living in the pink: Intentionality,

- Wellbeing, and Complexity. In C. A. Hooker (Eds), *Philosophy of Complex Systems: Handbook of the Philosophy of Science* (pp. 639-682). Amsterdam: Elsevier.
- von Holst, E. (1939/1973). On the nature of order in the central nervous system. In: R. Martin (Ed. and trans.), *The collected papers of Erich von Holst, vol. 1. The behavioral physiology of animal and man*. Coral Gables, FL: University of Miami Press.
- Vorberg, D., & Schulze, H. H. (2002). Linear phase-correction in synchronization: Predictions, parameter estimation, and simulations. *Journal of Mathematical Psychology*, *46*, 56-87.
- Wagenmakers, E. J., Farrell, S., & Ratcliff, R. (2004). Estimation and interpretation of  $1/f^\alpha$  noise in human cognition. *Psychonomic Bulletin & Review*, *11*, 579-615.
- Wagenmakers, E. J., Farrell, S., & Ratcliff, R. (2005). Human cognition and a pile of sand: a discussion on serial correlations and self-organized criticality. *Journal of Experimental Psychology: General*, *134*, 108-116.
- Ward, L. M. (2002). *Dynamical cognitive science*. Cambridge, MA: MIT Press.
- Wijnants, M. L. (2014). A review of theoretical perspectives in cognitive science on the presence of scaling in coordinated physiological and cognitive processes. *Journal of Nonlinear Dynamics*, 2014, Article ID 962043, 17 pages.
- Wijnants, M. L., Bosman, A. M., Hasselman, F., Cox, R. F., & Van Orden, G. C. (2009).  $1/f$  scaling in movement time changes with practice in precision aiming. *Nonlinear Dynamics, Psychology, and Life Sciences*, *13*, 75-94.
- Wijnants, M., Cox, R., Hasselman, F., Bosman, A., & Van Orden, G. (2012). A trade-off study revealing nested timescales of constraint. *Frontiers in physiology*, *3*, 116.
- Wing, A. M., & Kristofferson, A. B. (1973). Response delays and the timing of discrete motor responses. *Perception & Psychophysics*, *14*, 5-12.
- Winfree, A. T. (2001). *The geometry of biological time* (Vol. 12). Springer Science & Business Media.
- Zbilut, J. P., Giuliani, A., & Webber, C. L. (1998). Detecting deterministic signals in exceptionally noisy environments using cross-recurrence quantification. *Physics Letters A*, *246*, 122-128.
- Zelaznik, H. N., Spencer, R. M., & Ivry, R. B. (2008). Behavioral analysis of human movement timing. *Psychology of time*, 233-260.